GPLD1 is as a scavenger carrier mediating lysosomal degradation of extracellular aberrant proteins

Mizuki Tsuchiya[1], Yoichiro Yagishita[2], Akira Matsuura[3], Eisuke Itakura[345*]

[1] Department of Biology, Graduate school of Science and Engineering, Chiba University, Chiba, Japan

[2] Department of Biology, Faculty of Science, Chiba University, Chiba, Japan

[3] Department of Biology, Graduate School of Science, Chiba University. Chiba, Japan

[4] Center of Quantum Life Science for Structural Therapeutics (cQUEST), Chiba University, Chiba, Japan

[5] Institute for Advanced Academic Research (IAAR), Chiba University, Chiba, Japan

Abstract

Loss of proteostasis leads to the accumulation of aberrant proteins, including aggregated proteins and amyloid fibrils, contributing to various diseases. Protein quality control systems are essential for maintaining proteostasis. Although intracellular mechanisms are well characterized, pathways responsible for degradation of aberrant proteins outside the cell remain poorly understood. We previously identified the chaperone/carrier- and receptor-mediated extracellular protein degradation (CRED) pathway, in which the extracellular chaperone clusterin binds misfolded proteins and the resulting complex is delivered to lysosomes via endocytosis. However, it remains unclear whether other factors are involved in this pathway.

To identify novel regulators, plasma factors binding serum amyloid A1 (SAA1) were investigated. Glycosylphosphatidylinositol-specific phospholipase D1 (GPLD1) was found to directly bind SAA1 and promote its lysosomal degradation. This activity was independent of GPLD1's cleavage activity for GPI-anchored proteins. Furthermore, GPLD1 mediates lysosomal degradation of misfolded proteins, with cell surface heparan sulfate acting as its receptor. Our data demonstrate that GPLD1 is a novel scavenger carrier with substrate specificity distinct from clusterin, responsible for degrading extracellular aberrant proteins.

Keywords

Protein quality control system, Proteostasis, Lysosome, Aberrant protein, Protein degradation, Extracellular chaperone

Introduction

The accumulation of aberrant proteins leads to the formation of aggregates, which underlies the pathogenesis of various neurodegenerative diseases (Hipp *et al*, 2019; Tyedmers *et al*, 2010). For instance, amyloid fibrils, composed of β-sheet-rich proteins, deposit in tissues and cause a condition known as amyloidosis (Sawaya *et al*, 2021). To maintain proteostasis, cells rely on intracellular protein quality control systems, including autophagy and the ubiquitin-proteasome system, which degrade misfolded or damaged proteins (Klionsky *et al*, 2021; Wolff *et al*, 2014). The cytoplasm is densely populated with proteins, reaching concentrations of approximately 200–300 g/L. Similarly, extracellular compartments, such as the bloodstream, also exhibit high protein concentrations at approximately 80 g/L (Ellis, 2001). Although intracellular protein quality control mechanisms are well-characterized (Rusilowicz-Jones *et al*, 2022), the pathways responsible for the clearance of aberrant proteins in the extracellular environment remain poorly understood (Wyatt *et al*, 2013). In our previous study, we identified a novel pathway termed chaperone/carrier-mediated extracellular protein degradation (CRED) (Itakura *et al*, 2020). In this pathway, the extracellular chaperone clusterin recognizes and binds misfolded proteins, forming a complex that is subsequently internalized and selectively degraded in lysosomes via the cell surface heparan sulfate (HS) receptor. Clusterin also facilitates lysosomal degradation of amyloid β, a prototypical amyloidogenic protein (Calero *et al*, 2000; Itakura *et al.*, 2020). This mechanism contributes to the clearance of misfolded proteins from the extracellular environment (Itakura *et al.*, 2020). We have also found that α2-macroglobulin facilitates lysosomal degradation of extracellular aberrant proteins (Tomihari *et al*, 2023). However, the involvement of additional proteostasis regulators in the CRED pathway remains incompletely understood. In the present study, we investigated the existence of a novel CRED factor responsible for the degradation of extracellular amyloidogenic proteins. Amyloidosis is a pathological condition characterized by the extracellular deposition of insoluble, fibrillar proteins (amyloid fibrils), which leads to progressive organ dysfunction (Louros *et al*, 2023). In humans, more than 30 proteins have been identified as precursors of amyloid fibrils (Sipe *et al*, 2016). Serum amyloid A (SAA) is one such protein, strongly associated with amyloidosis and often arising as a complication of chronic inflammatory diseases. These conditions are marked by the deposition of insoluble amyloid fibrils in affected organs and tissues (Sun & Ye, 2016). Amyloid A (AA) amyloidosis specifically results from prolonged inflammation, which drives sustained overproduction of SAA1. This overproduction ultimately leads to the aggregation and deposition of AA amyloid in tissues (Gaffney, 2017). Human SAA1 is encoded by one of four SAA genes. Among these, SAA1 and SAA2 are acute-phase genes that are transcriptionally upregulated in response to inflammatory cytokines, which are induced by infections or autoimmune diseases. These proteins play roles in modulating cytokine synthesis and neutrophil chemotaxis (Uhlar & Whitehead, 1999). Consequently, identifying mechanisms responsible for the degradation of SAA1 in the bloodstream is of critical importance for prevention and mitigation of amyloidosis and related inflammatory conditions. Glycosylphosphatidylinositol-specific phospholipase D1 (GPLD1) is a secreted protein of approximately 110 kDa, predominantly produced by the liver (LeBoeuf *et al*, 1998). It possesses a catalytic site that cleaves the lipid-binding domain of glycosylphosphatidylinositol (GPI)-anchored proteins, which are exposed on the extracellular surface of the cell membrane. This enzymatic activity facilitates the release of GPI-anchored proteins from

the cell surface (Cao *et al*, 2023). Recent studies have shown that plasma levels of GPLD1 increase following physical exercise (Horowitz *et al*, 2020; Ren *et al*, 2024). Moreover, the exogenous expression of GPLD1 in aged mice has been reported to enhance cognitive function (Horowitz *et al.*, 2020). In this study, we identified GPLD1 as a plasma factor that binds SAA1, using mass spectrometry-based analysis. By developing an internalization assay using fluorescently tagged GPLD1, we demonstrated that GPLD1 promotes lysosomal degradation of SAA1 and other misfolded proteins. Mechanistically, HS functions as a cell surface receptor that mediates internalization of the GPLD1–aberrant protein complex. Notably, GPLD1 exhibited greater internalization activity toward SAA1 than clusterin, suggesting that SAA1 is a physiological substrate of GPLD1. These findings indicate that GPLD1 possesses distinct substrate specificity compared to the known extracellular chaperone clusterin and functions as a novel scavenger carrier involved in the clearance of extracellular aberrant proteins.

Results

GPLD1 binds SAA1 in plasma proteins

To identify novel extracellular proteostasis regulators, we analyzed SAA1-binding proteins from bovine plasma, which is rich in extracellular proteins, using His-ALFA-tagged SAA1-N as bait; this bait consists of the N-terminal 76 amino acid residues, which represent the core amyloidogenic fragment of SAA1(Liberta *et al*, 2019; Westermark *et al*, 1992). Given the amyloidogenic nature of SAA1-N, ALFA-SAA1-N was purified from *Escherichia coli* under denaturing conditions in the presence of urea. Note that SAA1-N was prepared in 8M urea-denatured form for all experiments. We confirmed that subsequent incubation of this denatured SAA1-N in PBS successfully induced the formation of protein aggregates (Fig. S1A). The purified ALFA-SAA1-N protein was then incubated with bovine plasma (The carry-over concentration of urea from the SAA1-N stock was kept below 0.05 M in the final incubation medium) and subjected to immunoprecipitation using ALFA nanobody-conjugated beads. Ruby staining revealed a range of proteins bound to ALFA-SAA1-N (Fig. S1B), and these were subsequently identified by mass spectrometry (Table S1). Notably, clusterin and apolipoprotein E—both known to interact with extracellular aberrant proteins—were among the identified proteins (Mahley *et al*, 2009; Matsubara *et al*, 1996), suggesting that this dataset may contain previously unrecognized extracellular proteostasis regulators involved in proteostasis. After excluding well-characterized proteins (APOB, APMAP, PLA2G7, GSN, VTN, COL6A3, COL18A1, and C9), we shortlisted seven candidate proteins (GPLD1, AHSG, APOD, SERPIND1, SERPINA10, SERPINF2, and SPP2) as potential extracellular proteostasis regulators. We then examined whether these candidates were internalized in cells in an SAA1-N-dependent manner and subsequently degraded in lysosomes. To detect lysosomal uptake of the candidates, we developed an internalization assay employing tandem-tagged constructs comprising red fluorescent protein (RFP:mCherry), green fluorescent protein (GFP:sfGFP), and a His-tag. RFP is highly resistant to lysosomal proteases and acidic pH, whereas GFP is more susceptible to degradation. Therefore, upon internalization and trafficking of RFP-GFP-His-tagged candidates into lysosomes, only the RFP portion accumulates, whereas the GFP signal is lost (Fig. 1A). The RFP-GFP-His (RG)-tagged candidate proteins were overexpressed in Flp-In T-REx HEK293 cells. The conditioned medium containing RG-tagged fusion proteins was collected and purified using His-tag affinity chromatography. For the internalization assay, ALFA-SAA1-N was mixed with serum-free medium containing the RG-tagged fusion protein and incubated at 37 °C for 2 h before being added to cultured cells. After 18 h of incubation, the cells were harvested, and GFP and RFP fluorescence intensities were measured using flow cytometry. The internalization assay revealed that one candidate, GPLD1-RG, exhibited an SAA1-N-dependent increase in RFP fluorescence intensity (Fig. 1B and C). Internalization of GPLD1-RG positively correlates with the dose of SAA1-N (Fig. S1C). Given that the SAA1-N stock solution contains 8 M urea, resulting in a final assay concentration of less than 50 mM, we tested the impact of 50 mM urea on GPLD1-RG uptake. Control experiments showed that the presence of 50 mM urea did not alter GPLD1-RG internalization (Fig. S2A), confirming that the residual urea does not interfere with the assay results. To investigate whether GPLD1-RG undergoes lysosomal degradation, cells were treated with bafilomycin A1 (BafA). BafA is a well-known inhibitor of lysosomal acidification that also affects endocytic trafficking (Baravalle *et al*, 2005). Consistent with its dual role in inhibiting both

endocytosis and lysosomal function, BafA treatment led to a marked reduction in albumin internalization (Fig. S2B) BafA treatment suppressed the SAA1-N-dependent increase in RFP accumulation, whereas GFP intensity increased (Fig. 1C), suggesting that the lysosomal trafficking of GPLD1-RG is inhibited. We further verified the lysosomal degradation of GPLD1-RG biochemically using an RFP cleavage assay (Tomihari *et al*, 2021). This assay detects the release of free 25-kDa RFP fragments generated from lysosomal digestion of the 160-kDa GPLD1-RG fusion protein. Free RFP was detected in cells treated with GPLD1-RG (Fig. 1D), and the amount of free RFP increased in the presence of SAA1-N. Notably, this increase was attenuated by BafA treatment. We investigated whether GPLD1 targets SAA1 during its denaturation process or after it has formed aggregates. To this end, GPLD1-RG was either mixed with ALFA-SAA1-N simultaneously or added to ALFA-SAA1-N that had been pre-incubated alone in the medium (Fig. S2C). Internalization assays revealed that pre-incubated SAA1-N was internalized at levels comparable to those observed under the simultaneous mixing condition. These results suggest that GPLD1 is involved in the internalization of aggregated SAA1. These results indicate that the GPLD1–SAA1-N complex is internalized and subsequently degraded in lysosomes.

GPLD1 binds aberrant proteins

To investigate whether GPLD1 directly interacts with substrate proteins, we conducted immunoprecipitation assays using recombinant proteins. Denatured ALFA-SAA1-N or native ALFA-SAA1-F (full-length) was incubated with GPLD1-RG, followed by immunoprecipitation using ALFA nanobody-conjugated beads. GPLD1 was found to co-immunoprecipitate with ALFA-SAA1-N and -F (Fig. 2A). To assess binding in the context of protein misfolding, we employed luciferase as a model substrate as it undergoes heat-induced denaturation at 42°C (Glover & Lindquist, 1998; Rodrigo-Brenni *et al*, 2014). Immunoprecipitation revealed that the association between GPLD1-RG and luciferase was enhanced under conditions promoting misfolding (Fig. 2B). These findings demonstrate that GPLD1 directly binds aberrant and misfolded proteins.

We further tested if GPLD1 facilitates the uptake of native SAA1-F. Surprisingly, GPLD1-RG internalization was not stimulated by either native or denatured ALFA-SAA1-F (Fig. S3A). Sedimentation analysis revealed that unlike denatured SAA1-N, which readily transitioned to the pellet fraction, SAA1-F (both native and denatured) showed negligible aggregation in PBS (Fig. S3B). This demonstrates the low aggregability of full-length SAA1. These data suggest that binding to GPLD1 does not, per se, trigger internalization; rather, the formation of SAA1 aggregates appears to be required for GPLD1-mediated transport to the lysosome.

We evaluated whether GPLD1 suppresses SAA1-N aggregation to determine its role as an extracellular chaperone. While GPLD1-RG exhibited a modest inhibitory effect on aggregation, this reduction did not reach statistical significance compared to the albumin control (Fig. S3C). These findings imply that instead of acting as a classic holdase chaperone, GPLD1 functions as a scavenger carrier by facilitating the clearance of SAA1 aggregates via the lysosomal pathway.

GPLD1 and the aberrant protein complex is degraded by lysosomes

To investigate lysosomal degradation mediated by GPLD1, we conducted an internalization assay

using serum-free medium containing GPLD1-RG and various substrate proteins. S-formylglutathione hydrolase (ESD), a substrate for the extracellular chaperones clusterin and α2-macroglobulin (α2M), has also been identified as a misfolded protein substrate (Tomihari *et al.*, 2023). GPLD1-RG was mixed with luciferase or ALFA-tagged ESD (ALFA-ESD) in serum-free medium. The luciferase mixture was denatured at 42°C for 30 min, whereas the ALFA-ESD mixture was denatured at 50°C for 1 h to induce misfolding. After replacing the cell culture medium with medium containing the GPLD1-RG–substrate mixtures, cells were incubated overnight and subsequently analyzed by flow cytometry. Compared to the GPLD1-RG–only controls, the addition of luciferase or ALFA-ESD significantly increased RFP intensity (Fig. 3A). As negative control experiments, heat stress alone (at either 42°C or 50°C) had no effect on the internalization of GPLD1-RG (Fig. S4A). Furthermore, GPLD1-RG is not coprecipitated with denatured luciferase, SAA1-N, ESD, or heat stress (Fig. S4B, C). These data suggest that GPLD1-RG promotes the lysosomal degradation of these misfolded proteins.

To examine the subcellular localization of GPLD1, we performed double immunostaining using a GPLD1 construct fused to Gamillus, a GFP resistant to lysosomal degradation (GPLD1-Gamillus-His) (Shinoda *et al*, 2018). Cells were treated as described in Fig. 1B and 3A with GPLD1-Gamillus, followed by immunostaining with an anti-LAMP1 antibody, a marker of the lysosomal membrane (Fig. 3B). In cells treated with GPLD1-Gamillus alone, green fluorescence was barely detectable. Conversely, the presence of luciferase or ALFA-SAA1-N markedly increased both the number and intensity of green fluorescent puncta. These GPLD1-Gamillus puncta co-localized with LAMP1-positive red signals, indicating lysosomal localization. Treatment with BafA suppressed the accumulation of RFP, but not GFP, in cells treated with GPLD1-RG and luciferase (Fig. 3C). Additionally, RFP cleavage assays demonstrated that BafA inhibits the increase of free RFP in cells exposed to GPLD1-RG and SAA1-N (Fig. 3D). These combined cell biological and biochemical findings suggest that the GPLD1–aberrant protein complex is internalized and trafficked to the lysosomal lumen for degradation.

Vascular endothelial cells exhibit higher levels of internalization of GPLD1 complex

We performed GPLD1-RG internalization assays in four cell lines of distinct tissue origins: HepG2 (liver carcinoma), U2OS (osteosarcoma), T98G (glioblastoma), and HuEhT (immortalized human vascular endothelial cells). Although no significant increase was observed with luciferase in any cell type, substrate-dependent internalization of GPLD1-RG was enhanced in most cell lines, with the exception of HepG2 cells (Fig. S5). Notably, the most substantial increase was detected in the vascular endothelial cell line HuEhT. In contrast, HepG2 cells exhibited no significant increase in GPLD1-RG internalization across all tested substrates. These results suggest that while GPLD1 is secreted from the liver, it mediates the degradation of extracellular proteins with a certain degree of tissue specificity.

Catalytic activity of GPLD1 is not required for internalization of the GPLD1 complex

GPLD1 exhibits catalytic activity that specifically hydrolyzes the inositol phosphate bond of GPI-

anchored proteins on the cell membrane (Cao *et al.*, 2023). Mutations at His133 or His158 abolish this enzymatic activity (Raikwar *et al*, 2005). To determine whether GPLD1's catalytic function is required for substrate-dependent intracellular uptake, we generated two catalytically inactive mutants—GPLD1-H133N-RG and GPLD1-H158N-RG—by substituting histidine residues at positions 133 and 158 with asparagine. Internalization assays revealed that these mutants did not significantly reduce RFP accumulation compared to wild-type GPLD1 (Fig. 4A). Given that these mutations effectively eliminate enzymatic activity (Horowitz *et al.*, 2020), yet internalization still occurred, these findings indicate that GPLD1's catalytic activity is not essential for substrate-mediated uptake. To further investigate whether GPI-anchored proteins are involved in GPLD1 internalization, we generated GPAA1 knockout (KO) cells. GPAA1 is a critical GPI transamidase required for the synthesis of GPI-anchored proteins (Eisenhaber *et al*, 2014). Western blot analysis confirmed the absence of GPAA1 protein in KO cells (Fig. 4B), and trafficking of GFP-tagged GPI-anchored proteins to the plasma membrane was disrupted in these cells (Fig. 4C), confirming the loss of surface GPI-anchored proteins. Nevertheless, GPLD1-RG internalization was not impaired in GPAA1 KO cells, as confirmed by flow cytometry and RFP cleavage assays, respectively (Fig. 4D and E), suggesting that uptake of the GPLD1–substrate complex occurs independently of GPI-anchored proteins.

Cell surface HS facilitates GPLD1 internalization

Nearly all vertebrate cells express a limited set of cell-surface HS proteoglycans, which serve as receptors for various growth factors and viruses (Liu & Thorp, 2002; Pillay *et al*, 2016; Xu & Esko, 2014; Yayon *et al*, 1991). In addition, HS functions as a membrane receptor for the substrate-dependent internalization of clusterin (Itakura *et al.*, 2020). To investigate whether HS is similarly involved in the substrate-dependent uptake of GPLD1, we first examined the potential direct interaction between GPLD1 and HS. A pulldown assay was performed using heparin-coated beads, which mimic the structure of HS chains. GPLD1-RG, but not the RG tag alone, was precipitated by the heparin-coated beads (Fig. 5A), indicating a specific interaction. Furthermore, this binding was competitively inhibited by the addition of free heparin.

We conducted GPLD1-RG internalization assays using EXT1 KO cells, which lack EXT1, an essential enzyme for the biosynthesis of HS (McCormick *et al*, 1998). In these cells, the luciferase-induced increase in RFP levels was reduced to less than half compared to wild-type cells and EXT1 overexpression (EXT1 OE) cells (Fig. 5B). Notably, overexpression of EXT1 in KO (EXT1 OE-EXT1 KO) cells restored RFP intensity, suggesting that HS biosynthesis is critical for GPLD1-RG internalization. To further examine the direct role of extracellular HS in this process, we performed a competitive inhibition assay using free heparin. GPLD1-RG was mixed with luciferase or ALFA-SAA1-N in serum-free medium and incubated with cells in the presence or absence of excess heparin. The addition of heparin significantly reduced GPLD1-RG internalization, lowering uptake to less than half of the original level (Fig. 5C). Collectively, these results indicate that cell-surface HS mediates substrate-dependent internalization of GPLD1.

Substrate selectivity of GPLD1 differs from that of clusterin

To compare the substrate selectivity of GPLD1 with that of clusterin, we performed internalization

assays using clusterin-RG and GPLD1-RG at equal concentrations. Three types of substrate proteins were tested: luciferase, ALFA-SAA1-N, and amyloid β 1-42 (Aβ42)-ALFA. Clusterin-RG induced the highest increase in RFP intensity in the presence of Aβ42, whereas its response to SAA1-N was comparatively lower. Conversely, GPLD1-RG showed a greater increase in RFP intensity with SAA1-N than with Aβ42 (Fig. 6A). To determine if substrate-selective uptake correlates with binding, immunoprecipitation assays were performed. We found that GPLD1 preferentially binds to SAA1-N over Ab42, while clusterin showed the opposite binding profile (Fig. 6B). These results suggest that GPLD1 exhibits a substrate selectivity profile distinct from that of clusterin.

Discussion

We previously identified the CRED pathway, in which extracellular chaperones such as clusterin bind aberrant proteins, forming complexes that are selectively internalized via specific cell-surface receptors and subsequently degraded in lysosomes, thereby facilitating the removal of aberrant proteins from the extracellular space (Itakura *et al.*, 2020; Tomihari *et al.*, 2023). In the present study, we identified GPLD1 as a novel extracellular scavenger carrier. Co-immunoprecipitation of purified GPLD1 demonstrated its ability to directly interact with SAA1-N and misfolded proteins (Fig. 2). Internalization assays using GPLD1-RG showed that GPLD1 mediates the cellular uptake of both SAA1-N and misfolded proteins (Fig. 3A). We further confirmed that this internalization leads to lysosomal degradation, as evidenced by fluorescence microscopy and RFP cleavage assays (Fig. 3B and 3C). Additionally, our data indicate that this process is dependent on cell-surface HS (Fig. 5). Collectively, these findings suggest that GPLD1 facilitates the selective lysosomal degradation of aberrant protein complexes through an HS-dependent mechanism at the cell surface (Fig. 6B).

SAA family proteins, including SAA1, are known to be upregulated in chronic inflammatory conditions such as metabolic syndrome, diabetes, and rheumatoid arthritis (Wilson *et al*, 2018). Elevated SAA1 expression has also been reported in the livers of patients with non-alcoholic fatty liver disease (Jiang *et al*, 2022). Similarly, GPLD1 expression is significantly increased in individuals with obesity, diabetes, and non-alcoholic fatty liver disease (Cao *et al.*, 2023). Considering the lysosomal uptake activity of GPLD1 demonstrated in this study, it is plausible that GPLD1 is upregulated to facilitate the degradation of elevated SAA1 during inflammatory responses. Although this study focused on amyloidosis-associated proteins to identify GPLD1, our findings show that GPLD1 is also effective in targeting misfolded proteins beyond amyloidogenic substrates. Therefore, GPLD1 may have potential therapeutic applications across a broad spectrum of protein misfolding-related diseases.

A comparison of substrate selectivity between GPLD1 and clusterin revealed that GPLD1 exhibits higher uptake activity for SAA1-N than clusterin (Fig. 6A), suggesting that SAA1 is a specific substrate of GPLD1. GPLD1 is primarily secreted by the liver and is present in the bloodstream at relatively high concentrations (approximately 40-160 μg/ml) (Bjelosevic *et al*, 2017; Qin *et al*, 2016). This high level may reflect its role in rapidly clearing aberrant proteins that arise in circulation. Although the liver is the main source of GPLD1 secretion, it is also expressed in the brain (Cao *et al.*, 2023). The presence of GPLD1 in the brain suggests a potential role in the uptake of amyloidosis-associated proteins, which may help prevent Alzheimer's disease. Supporting this, increased GPLD1 expression has been reported to reduce Aβ42 levels through interactions involving Galectin-3 binding protein (Seki *et al*, 2020), indicating an indirect connection between GPLD1 and amyloid pathology.

We investigated whether HS, known to serve as a cell surface receptor for clusterin, also plays a role in GPLD1 internalization. In EXT1 KO cells, which lack HS chains (McCormick *et al.*, 1998), substrate-dependent uptake of GPLD1 was significantly reduced (Fig. 5B). Additionally, the presence of heparin in the culture medium, which mimics HS chains, decreased GPLD1 internalization (Fig. 5C). However, internalization was not completely abolished in EXT1 KO cells (Fig. 5B), indicating that although HS chains are not essential receptors, they likely facilitate GPLD1 uptake at the cell surface. It is plausible that HS chains, due to their extended polysaccharide structure, tether

305 extracellular GPLD1 and may transfer it to an as-yet unidentified cell surface receptor. Indeed, HS
306 chains function as receptors for fibroblast growth factor 2 (FGF2), enhancing its binding to the FGF2
307 receptor (Nadanaka & Kitagawa, 2018; Xu & Esko, 2014). HS chains are a major constituent of the
308 glycocalyx, which is highly abundant in vascular endothelial cells (Reitsma *et al*, 2007). Consistent
309 with this, our data demonstrated that GPLD1-RG internalization was highest in the vascular
310 endothelial cell line, HuEhT (Fig. S5). While heparan sulfate serves as a primary tethering factor, its
311 relative abundance across different tissues may act as a key regulatory mechanism for determining the
312 tissue-specific uptake of the GPLD1-substrate complex. Although the GPLD1-substrate complex is
313 selectively internalized upon substrate binding, the mechanism by which endocytosis is preferentially
314 promoted for this complex rather than GPLD1 alone remains unclear. We propose that binding of
315 aberrant proteins induces a conformational change in GPLD1, enabling interaction with an unknown
316 cell surface receptor that mediates internalization. Future studies aimed at identifying this receptor
317 will be crucial to fully understand GPLD1-mediated uptake.
318 GPLD1 exhibits enzymatic activity that cleaves the lipid-binding site of GPI-anchored proteins
319 exposed on the cell surface, thereby releasing them from the membrane (Cao *et al.*, 2023). These
320 released GPI-anchored proteins are thought to influence chronic diseases by modulating various
321 metabolic pathways (Cao *et al.*, 2023). To explore the relationship between GPLD1's enzymatic
322 activity and its internalization, we generated catalytic mutants and conducted internalization assays.
323 The GPLD1 H133N and H158N mutants, which display nearly undetectable enzymatic activity in
324 biochemical assays (Raikwar *et al.*, 2005), retained their ability to undergo internalization (Fig. 4A),
325 indicating that enzymatic activity is not essential for this process. Additionally, internalization assays
326 using cells deficient in GPI-anchored proteins confirmed that GPLD1 internalization occurs
327 independently of these proteins (Fig. 4B). Notably, GPLD1's enzymatic function has been shown to
328 be required for cognitive improvements in mice (Horowitz *et al.*, 2020). Thus, GPLD1 appears to be
329 a bifunctional molecule, both cleaving GPI-anchored proteins and facilitating the degradation of
330 aberrant proteins. Given that the accumulation of aberrant proteins is linked to impaired brain function
331 (Currais *et al*, 2017), GPLD1 may contribute to neural health through a synergistic mechanism
332 involving both its enzymatic activity and its role in aberrant protein internalization.
333 Molecular chaperones were originally defined as factors that assist in protein folding.
334 Conversely, extracellular chaperones function primarily to maintain the solubility of abnormal proteins
335 by binding them directly and preventing aggregation in the extracellular environment (Wyatt *et al.*,
336 2013). Given the low ATP concentration outside the cell, extracellular chaperones lack refolding
337 activity. Indeed, extracellular chaperones such as clusterin do not possess ATPase domains (Poon *et*
338 *al*, 2000) but effectively inhibit stress-induced protein aggregation (Humphreys *et al*, 1999). Whether
339 GPLD1 can similarly prevent aggregate formation remains to be determined. Based on current
340 evidence, GPLD1 functions as a scavenger carrier that facilitates the lysosomal degradation of aberrant
341 proteins in the extracellular space. It exhibits distinct substrate selectivity from clusterin and operates
342 within the CRED pathway (Fig. 6B). Further investigation is needed to elucidate the molecular
343 mechanisms underlying GPLD1-mediated degradation of extracellular aberrant proteins, which may
344 inform novel therapeutic strategies for their removal. Recently, several lysosome-targeting chimeras
345 (LYTACs) have been developed to artificially degrade extracellular substrates by employing

346 bifunctional molecules that bind both the plasma membrane and the target protein (Banik *et al*, 2020;
347 Kim *et al*, 2024). However, because these chimeras are transported to lysosomes even in the absence
348 of substrate, repeated dosing may be required over time. Conversely, administration of scavenger
349 factors such as GPLD1 and clusterin may prove more efficient, as substrate binding triggers their
350 lysosomal transport. Therefore, a thorough understanding of the substrate recognition mechanism of
351 GPLD1 is critical to effectively target specific extracellular substrates. Collectively, our findings
352 provide valuable insights into extracellular proteostasis and advance the field of selective degradation
353 of extracellular aberrant proteins.
354

355 ## Methods
356
357 **Cell culture**
358 Flp-In T-Rex HEK293 cells (Thermo Fisher Scientific, Waltham, MA, USA; cat# R78007), HepG2
359 cells (RIKEN BRC, cat# RCB1648), and U2OS cells were cultured in Dulbecco's modified Eagle
360 medium (DMEM; Nacalai Tesque). T98G cells (JCRB, cat# IFO50303) were maintained in Eagle's
361 minimum essential medium (MEM; Nacalai Tesque). HuEhT-2 cells (JCRB, cat# JCRB1459) were
362 cultured in MCDB131 medium (Thermo Fisher Scientific) supplemented with 0.03 g/L endothelial
363 cell growth supplement (ECGS), 5 μg/mL heparin, and 10 mM L-glutamine. All media were further
364 supplemented with 10% fetal bovine serum (FBS; Biosera) and 50 μg/mL penicillin-streptomycin.
365 Cells were maintained in a humidified incubator at 37°C with 5% CO_2. To generate stable cell lines
366 with doxycycline-inducible expression of secreted proteins (e.g., GPLD1-mCherry-sfGFP-His), Flp-
367 In T-Rex HEK293 cells were co-transfected with plasmids encoding the proteins of interest and
368 pOG44, which encodes FLP recombinase. Transfected cells were selected and maintained in medium
369 containing 100 μg/mL hygromycin. Gene expression at the FRT site was induced by treatment with
370 200 ng/mL doxycycline (Clontech).
371
372 **Plasmids**
373 To construct GPLD1-mCherry-sfGFP-His (GPLD1-RG) and GPLD1-Gamillus-His (GPLD1-
374 Gamillus), full-length human GPLD1 was amplified from total cDNA extracted from HepG2 cells by
375 PCR. Gamillus was amplified from pcDNA3-Gamillus (a gift from Dr. Takeharu Nagai, Osaka
376 University) (Shinoda *et al.*, 2018). The amplified cDNAs were cloned into the pcDNA5 FRT TO vector
377 along with sequences encoding mCherry, sfGFP, Gamillus, and a His-tag to generate pcDNA5 FRT
378 TO GPLD1-RG and GPLD1-Gamillus constructs. GPLD1 mutants (H133N, H158N) were generated
379 via site-directed mutagenesis. The pcDNA5 FRT TO clusterin-mCherry-sfGFP-His (clusterin-RG)
380 construct was described previously (Itakura *et al.*, 2020). The pOG44 plasmid was used for the Flp-In
381 recombination system. For the generation of His-ALFA-SAA1-N terminus (SAA1-N) (human SAA1
382 19-94 amino acids), His-ALFA-SAA1-Full length (SAA1-F)(human SAA1 19-122 amino acids), and
383 Ab42 (amyloid β1-42)-ALFA-His, SAA1 and Ab42 sequences were synthesized as gBlock Gene
384 Fragments (Integrated DNA Technologies, Coralville, IA, USA). These fragments were inserted into
385 the pRSET-A vector along with ALFA-tag and His-tag sequences to produce pRSET-A His-ALFA-
386 SAA1-N, His-ALFA-SAA1-F, and pRSET-A Ab42-ALFA-His. To construct pCW SS-RFP-GFP-GPI,
387 the signal sequence of prolactin, mCherry, sfGFP, and a 78-bp GPI-anchor sequence derived from
388 prion protein were subcloned into the pCW57.1 vector (Addgene, cat# 41393). Lentiviral packaging
389 plasmids pCMV-VSVG (Addgene, cat# 8454) and psPAX2 (Addgene, cat# 12260) were used for
390 lentivirus production.
391
392 **Generation of KO cells**
393 EXT1 KO cells were generated as previously described (Itakura *et al.*, 2020). To create GPAA1 KO
394 cells, a GPAA1-targeting sgRNA (CCTCTTACCGGTGGGTATTG) was cloned into lentiCRISPRv2
395 hygro (Addgene, cat#98291). HeLa cells were infected with lentivirus carrying Cas9 and the GPAA1

396 sgRNA. After 24 h, cells were selected with 100 μg/mL hygromycin for over 7 days, followed by
397 cloning via limiting dilution.
398
399 **Antibodies**
400 Rabbit polyclonal anti-LAMP1 antibody was kindly provided by Y. Tanaka (Kyushu University,
401 Fukuoka, Japan). Rabbit polyclonal antibodies against sfGFP, mCherry, and the ALFA tag were
402 generated by Eurofins using full-length mCherry protein and the ALFA peptide as antigens. Rabbit
403 polyclonal anti-luciferase antibody (cat# PM016) was purchased from MBL. Rabbit polyclonal anti-
404 β-actin (cat# 20536-1-AP) and anti-GPAA1 (cat# 10104-1-AP) antibodies were obtained from
405 Proteintech. HRP-conjugated anti-rabbit antibody (cat# 7074S) was purchased from Cell Signaling
406 Technology.
407 ALFA nanobody beads were prepared by conjugating ALFA nanobody protein (Götzke *et al*,
408 2019), purified from pRSET-A ALFA-His, to N-hydroxysuccinimide (NHS)-activated Sepharose 4
409 Fast Flow (GE). Similarly, GFP nanobody beads were prepared by conjugating GFP nanobody protein,
410 purified from the pOPINE GFP nanobody plasmid (Addgene #49712), to NHS-activated Sepharose 4
411 Fast Flow (GE).
412
413 **Recombinant proteins from *E. coli***
414 Recombinant luciferase was purchased from Promega (cat# E1701). His-ALFA-SAA1 and Ab42-
415 ALFA-His were cloned into the pRSET-A vector and expressed in *E. coli* BL21(DE3) pLysS (Promega,
416 cat# L1191). After harvesting, *E. coli* cells were disrupted by sonication. Following ultracentrifugation
417 at 200,000 × *g* for 30 min at 4°C, the inclusion bodies (pellet fraction) containing His-ALFA-SAA1-
418 N or Ab42-ALFA-His were solubilized by sonication in urea buffer (8 M urea, PBS, 10 mM imidazole).
419 To remove insoluble debris, the soluble fraction was subjected to ultracentrifugation at 200,000 × *g*
420 for 30 min at 4°C. The resulting supernatant was purified using Co-NTA affinity chromatography
421 under denaturing conditions (8 M urea, PBS). After elution using 200 mM imidazole buffer, purified
422 His-ALFA-SAA1-N and Ab42-ALFA-His were stored in the presence of urea. His-ALFA-ESD was
423 described previously (Tomihari *et al.*, 2023).
424
425 **Recombinant proteins from mammalian cells**
426 For secreted proteins from mammalian cells, pcDNA5 FRT TO plasmids encoding GPLD1-RG-His,
427 GPLD1-Gamillus-His, and Clusterin-RG-His were integrated into the FLP site of the genome in Flp-
428 In T-Rex293 cells to generate stable (Tet-on) cell lines. Purification of secreted proteins from
429 conditioned medium was performed as previously described (Tomihari *et al.*, 2021). Briefly, cells were
430 cultured for 4 days in serum-free Advanced DMEM/F12 medium (Thermo Fisher Scientific, cat#
431 12634010) supplemented with L-glutamine and 0.2 μg/mL doxycycline. The culture supernatant was
432 collected and centrifuged at 3500 rpm for 10 min at 4°C to remove dead cells. Secreted proteins were
433 purified from the conditioned medium using Ni-NTA affinity chromatography. After elution using 200
434 mM imidazole buffer, the purified proteins were stored in PBS containing 10% glycerol.
435
436 **Internalization assay**

437 Purified GPLD1-RG wild-type or mutant (0.2 μM) or clusterin-RG (0.2 μM) in serum-free Advanced
438 DMEM/F12 medium or serum-free conditioned medium containing secreted GPLD1-RG was mixed
439 with substrate proteins. It should be noted that while Advanced DMEM/F12 is serum-free, it is
440 supplemented with specific proteinaceous growth factors, including albumin (400 mg/L), insulin (10
441 mg/L), and transferrin (7.5 mg/L). The mixtures were incubated as follows: luciferase (0.2 μM) was
442 heat-treated at 42°C for 30 min; His-ALFA-ESD (8 μM) was heat-treated at 50°C for 1 h; and His-
443 ALFA-SAA1 (8 μM) and Ab42-ALFA-His (8 μM) were incubated at 37°C with shaking for 2 h. After
444 incubation, protein aggregates were removed by centrifugation at 15,000 rpm for 5 min . Cells were
445 then cultured with the resulting supernatant (serum-free medium containing extracellular protein-RG
446 with or without substrate) at 37°C for 18 h. In specified experiments, 0.1 μM BafA (LC Laboratories)
447 or 80 μg/mL heparin (Nacalai Tesque) was added together with the medium. Cells were detached using
448 trypsin, and subsequently analyzed by flow cytometry and immunoblotting. For immunostaining, cells
449 were pre-cultured on glass coverslips.
450
451 **Flow cytometry**
452 Cells were detached using trypsin and resuspended in a solution containing 5% newborn calf serum
453 and 1 μg/mL 4′ ,6-diamidino-2-phenylindole (DAPI) in PBS. The cell suspension was then passed
454 through a 70 μm cell strainer and collected into a 1.5 mL tube. The collected cells were analyzed by
455 flow cytometry using a CytoFLEX S flow cytometer (Beckman Coulter) equipped with 375-nm
456 (DAPI), 488-nm (sfGFP), and 561-nm (mCherry) lasers. Cells were gated sequentially: first by FSC-
457 A/SSC-A for the target population, then by SSC-W/SSC-A to select singlets. DAPI staining was used
458 to exclude dead cells. Green and red fluorescence intensities were then measured in the remaining live
459 singlet cells, capturing a total of 10,000 events per sample. The Mean Fluorescence Intensity (MFI)
460 was used for analysis.
461
462 **Immunostaining and fluorescence microscopy**
463 HuEhT-2 cells cultured on coverslips were fixed at room temperature for 15 min with 3.7%
464 formaldehyde in PBS. For immunostaining, the fixed cells were permeabilized for 5 min with 50
465 μg/mL digitonin in PBS. After blocking with 10% newborn calf serum in PBS for 30 min, the cells
466 were incubated with the primary antibody for 1 h. Following three washes with PBS, cells were
467 incubated for 1 h with Alexa Fluor 568-conjugated goat anti-rabbit IgG antibody (Thermo Fisher
468 Scientific). The cells were then mounted with a DAPI/DABCO/Glycerol/PBS solution. Stained cells
469 were observed using a confocal laser scanning microscope (FV1000IX81; Olympus, Tokyo, Japan)
470 equipped with a 100× oil immersion lens (NA 1.40).
471
472 **Cell lysis and immunoblotting**
473 Cells were washed with cold PBS and lysed for 15 min at 4°C in lysis buffer containing 1% Triton X-
474 100, 50 mM Tris-HCl (pH 7.5), 1 mM EDTA, and 150 mM NaCl, supplemented with an EDTA-free
475 protease inhibitor cocktail (Nacalai Tesque) and 1 mM phenylmethanesulfonyl fluoride (PMSF). After
476 centrifugation at 20,000 × *g* for 5 min, the supernatant was collected, mixed with 6× SDS sample

477 buffer, and boiled at 95°C for 5 min. Proteins were separated by SDS-PAGE, transferred to a
478 polyvinylidene difluoride membrane (Millipore, cat# IPVH00010), and probed with antibodies diluted
479 in Signal Enhancer HIKARI (Nacalai Tesque, cat# 02270-81). Protein bands were visualized using
480 ImmunoStar Zeta (Fujifilm Wako Pure Chemical Industries, cat# 297-72404).
481
482 **Identification of SAA1-binding proteins**
483 ALFA-SAA1 (8 μM) was added to 50% bovine plasma (Rockland Immunochemicals, cat# D500-06-
484 0500) (in PBS) and incubated for 16 h at 4°C. The plasma was then centrifuged at 20,000 × *g* for 10
485 min to remove debris. The supernatant was mixed with ALFA-nanobody beads and rotated for 1 h at
486 4°C. The beads were washed four times with PBS, transferred to a new tube, mixed with SDS sample
487 buffer, and boiled for 5 min. Binding proteins were identified by LC-MS/MS proteomics(Toh *et al*,
488 2022).
489
490 **Immunoprecipitation**
491 Purified GPLD1-RG (final concentration: 10 nM for GFP IP, 40 nM for ALFA IP) and substrate
492 proteins (final concentration: 40 nM luciferase for GFP IP, 500 nM His-ALFA-SAA1 for ALFA IP)
493 were mixed in PBS and incubated at 4°C, except luciferase which was incubated at 42°C for 30 min
494 and His-ALFA-SAA1 at 37°C with shaking for 2 h. After incubation, excess protein aggregates were
495 removed by centrifugation at 20,000 × *g* for 5 min. The supernatant was collected; a portion was
496 reserved as the "input" sample, while the remainder was mixed with GFP nanobody or ALFA
497 nanobody beads (5 μL bed volume) and incubated at 4°C for 2 h. The beads were washed four times
498 with PBS, transferred to a new tube, mixed with SDS sample buffer, and boiled for 5 min.
499 For the pulldown assay using heparin beads, 30 nM GPLD1-RG or 30 nM RG was mixed with
500 heparin beads (M&S TechnoSystems, cat# Super-HEP10) in 0.04% BSA/PBS, in the presence or
501 absence of 80 μg/mL free heparin, and then rotated for 2 h at 4°C. The beads were washed four times
502 with PBS, transferred to a new tube, mixed with SDS sample buffer, and boiled for 5 min.
503
504 **Sedimentation assay**
505 For the sedimentation assays, SAA1 (8 μM for Fig. S1A and S3B), Albumin-ALFA (2 μM for Fig.
506 S1A and S3C), or GPLD1-RG (2 μM for Fig. S3C) in PBS or adDMEM/F12 was incubated for 2 h
507 at 37°C with shaking. Following incubation, the mixtures were centrifuged at 20,000 × *g* for 10 min
508 at 4°C. The supernatant was collected as the supernatant fraction, while the remaining pellet was
509 washed with PBS and subjected to a second centrifugation step at 20,000 × *g* for 10 min. The final
510 pellet was then collected as the pellet fraction for subsequent analysis.
511
512 **Statistical analysis**
513 Data were collected from at least three biological replicates ($n \geq 3$). One-way ANOVA with Dunnett's
514 post hoc test was used for significance testing in Figs. 1D, 2A, 3A, 3B, 3D, 5A, 5B, S1C, S2C, S3A,
515 S3C, S4A, and S5. One-way ANOVA with Tukey's post hoc test was used for Figs. 1C, 3C and 4A.
516 Welch's t-test was applied for Fig. 2B, 4E, 5C 6A, 6B, S2A, and S2B. In addition to significance
517 testing, effect sizes were calculated to quantify the magnitude of the observed effects. We used Cohen's

d, and interpreted values based on conventional guidelines: 0.2 for a small effect, 0.5 for a medium effect, and 0.8 for a large effect for Fig. 5 and 6.

Acknowledgments

This work was supported by JSPS KAKENHI (grant nos. 20H03249, 22H04634, 23H04932, 24K02018 to E.I.), the JST FOREST Program (grant no. JPMJFR204N to E.I.), the JSPS Program for Forming Japan's Peak Research Universities (J-PEAKS) (grant no. JPJS00420230002 to E.I.), and the Takeda Science Foundation (to E.I.). We thank Dr. Yoshitaka Tanaka (Kyushu University) for providing the anti-LAMP1 antibodies, Dr. Takeharu Nagai (Osaka University) for the pcDNA3 Gamillus plasmid, and Dr. Reiko Nakagawa (Laboratory for Cell-Free Protein Synthesis, RIKEN Center for Biosystems Dynamics Research) for conducting the mass spectrometry experiments.

Author contributions

Mizuki Tsuchiya: Formal analysis; Validation; Investigation; Visualization; Writing—original draf. **Yoichiro Yagishita:** Investigation; Formal analysis. **Akira Matsuura**: Writing—original draft; Writing—review and editing. **Eisuke Itakura**: Conceptualization; Formal analysis; Supervision; Investigation; Visualization; Funding acquisition; Writing—original draft; Project administration; Writing—review and editing

Competing interests

The authors declare no conflicts of interest.

540 **References**

541 Banik SM, Pedram K, Wisnovsky S, Ahn G, Riley NM, Bertozzi CR (2020) Lysosome-targeting
542 chimaeras for degradation of extracellular proteins. *Nature* 584: 291-297
543 Baravalle G, Schober D, Huber M, Bayer N, Murphy RF, Fuchs R (2005) Transferrin recycling
544 and dextran transport to lysosomes is differentially affected by bafilomycin, nocodazole, and low
545 temperature. *Cell Tissue Res* 320: 99-113
546 Bjelosevic S, Pascovici D, Ping H, Karlaftis V, Zaw T, Song X, Molloy MP, Monagle P, Ignjatovic
547 V (2017) Quantitative Age-specific Variability of Plasma Proteins in Healthy Neonates, Children
548 and Adults. *Mol Cell Proteomics* 16: 924-935
549 Calero M, Rostagno A, Matsubara E, Zlokovic B, Frangione B, Ghiso J (2000) Apolipoprotein J
550 (clusterin) and Alzheimer's disease. *Microsc Res Tech* 50: 305-315
551 Cao J, Zhou A, Zhou Z, Liu H, Jia S (2023) The role of GPLD1 in chronic diseases. *J Cell*
552 *Physiol* 238: 1407-1415
553 Currais A, Fischer W, Maher P, Schubert D (2017) Intraneuronal protein aggregation as a trigger
554 for inflammation and neurodegeneration in the aging brain. *FASEB J* 31: 5-10
555 Eisenhaber B, Eisenhaber S, Kwang TY, Grüber G, Eisenhaber F (2014) Transamidase subunit
556 GAA1/GPAA1 is a M28 family metallo-peptide-synthetase that catalyzes the peptide bond
557 formation between the substrate protein's omega-site and the GPI lipid anchor's
558 phosphoethanolamine. *Cell Cycle* 13: 1912-1917
559 Ellis RJ (2001) Macromolecular crowding: an important but neglected aspect of the intracellular
560 environment. *Curr Opin Struct Biol* 11: 114-119
561 Gaffney PM (2017) Amyloid A Amyloidosis. *Vet Pathol* 54: 5-8
562 Glover JR, Lindquist S (1998) Hsp104, Hsp70, and Hsp40: a novel chaperone system that
563 rescues previously aggregated proteins. *Cell* 94: 73-82
564 Götzke H, Kilisch M, Martínez-Carranza M, Sograte-Idrissi S, Rajavel A, Schlichthaerle T,
565 Engels N, Jungmann R, Stenmark P, Opazo F *et al* (2019) The ALFA-tag is a highly versatile tool
566 for nanobody-based bioscience applications. *Nat Commun* 10: 4403
567 Hipp MS, Kasturi P, Hartl FU (2019) The proteostasis network and its decline in ageing. *Nat*
568 *Rev Mol Cell Biol* 20: 421-435
569 Horowitz AM, Fan X, Bieri G, Smith LK, Sanchez-Diaz CI, Schroer AB, Gontier G, Casaletto
570 KB, Kramer JH, Williams KE *et al* (2020) Blood factors transfer beneficial effects of exercise on
571 neurogenesis and cognition to the aged brain. *Science* 369: 167-173
572 Humphreys DT, Carver JA, Easterbrook-Smith SB, Wilson MR (1999) Clusterin has chaperone-
573 like activity similar to that of small heat shock proteins. *J Biol Chem* 274: 6875-6881
574 Itakura E, Chiba M, Murata T, Matsuura A (2020) Heparan sulfate is a clearance receptor for
575 aberrant extracellular proteins. *J Cell Biol* 219

576 Jiang B, Wang D, Hu Y, Li W, Liu F, Zhu X, Li X, Zhang H, Bai H, Yang Q *et al* (2022) Serum
577 amyloid A1 exacerbates hepatic steatosis via TLR4-mediated NF-κB signaling pathway. *Mol*
578 *Metab* 59: 101462
579 Kim J, Byun I, Kim DY, Joh H, Kim HJ, Lee MJ (2024) Targeted protein degradation directly
580 engaging lysosomes or proteasomes. *Chem Soc Rev* 53: 3253-3272
581 Klionsky DJ, Petroni G, Amaravadi RK, Baehrecke EH, Ballabio A, Boya P, Bravo-San Pedro JM,
582 Cadwell K, Cecconi F, Choi AMK *et al* (2021) Autophagy in major human diseases. *EMBO J* 40:
583 e108863
584 LeBoeuf RC, Caldwell M, Guo Y, Metz C, Davitz MA, Olson LK, Deeg MA (1998) Mouse
585 glycosylphosphatidylinositol-specific phospholipase D (Gpld1) characterization. *Mamm Genome*
586 9: 710-714
587 Liberta F, Loerch S, Rennegarbe M, Schierhorn A, Westermark P, Westermark GT, Hazenberg
588 BPC, Grigorieff N, Fändrich M, Schmidt M (2019) Cryo-EM fibril structures from systemic AA
589 amyloidosis reveal the species complementarity of pathological amyloids. *Nat Commun* 10: 1104
590 Liu J, Thorp SC (2002) Cell surface heparan sulfate and its roles in assisting viral infections.
591 *Med Res Rev* 22: 1-25
592 Louros N, Schymkowitz J, Rousseau F (2023) Mechanisms and pathology of protein misfolding
593 and aggregation. *Nat Rev Mol Cell Biol* 24: 912-933
594 Mahley RW, Weisgraber KH, Huang Y (2009) Apolipoprotein E: structure determines function,
595 from atherosclerosis to Alzheimer's disease to AIDS. *J Lipid Res* 50 Suppl: S183-188
596 Matsubara E, Soto C, Governale S, Frangione B, Ghiso J (1996) Apolipoprotein J and
597 Alzheimer's amyloid beta solubility. *Biochem J* 316 (Pt 2): 671-679
598 McCormick C, Leduc Y, Martindale D, Mattison K, Esford LE, Dyer AP, Tufaro F (1998) The
599 putative tumour suppressor EXT1 alters the expression of cell-surface heparan sulfate. *Nat*
600 *Genet* 19: 158-161
601 Nadanaka S, Kitagawa H (2018) Exostosin-like 2 regulates FGF2 signaling by controlling the
602 endocytosis of FGF2. *Biochim Biophys Acta Gen Subj* 1862: 791-799
603 Pillay S, Meyer NL, Puschnik AS, Davulcu O, Diep J, Ishikawa Y, Jae LT, Wosen JE, Nagamine
604 CM, Chapman MS *et al* (2016) An essential receptor for adeno-associated virus infection.
605 *Nature* 530: 108-112
606 Poon S, Easterbrook-Smith SB, Rybchyn MS, Carver JA, Wilson MR (2000) Clusterin is an ATP-
607 independent chaperone with very broad substrate specificity that stabilizes stressed proteins in a
608 folding-competent state. *Biochemistry* 39: 15953-15960
609 Qin W, Liang YZ, Qin BY, Zhang JL, Xia N (2016) The Clinical Significance of Glycoprotein
610 Phospholipase D Levels in Distinguishing Early Stage Latent Autoimmune Diabetes in Adults
611 and Type 2 Diabetes. *PLoS One* 11: e0156959

612 Raikwar NS, Bowen RF, Deeg MA (2005) Mutating His29, His125, His133 or His158 abolishes
613 glycosylphosphatidylinositol-specific phospholipase D catalytic activity. *Biochem J* 391: 285-289
614 Reitsma S, Slaaf DW, Vink H, van Zandvoort MA, oude Egbrink MG (2007) The endothelial
615 glycocalyx: composition, functions, and visualization. *Pflugers Arch* 454: 345-359
616 Ren T, He J, Zhang T, Niu A, Yuan Y, Zuo Y, Miao Y, Zhang H, Zang L, Qiao C *et al* (2024)
617 Exercise activates interferon response of the liver via Gpld1 to enhance antiviral innate
618 immunity. *Sci Adv* 10: eadk5011
619 Rodrigo-Brenni MC, Gutierrez E, Hegde RS (2014) Cytosolic quality control of mislocalized
620 proteins requires RNF126 recruitment to Bag6. *Mol Cell* 55: 227-237
621 Rusilowicz-Jones EV, Urbé S, Clague MJ (2022) Protein degradation on the global scale. *Mol*
622 *Cell* 82: 1414-1423
623 Sawaya MR, Hughes MP, Rodriguez JA, Riek R, Eisenberg DS (2021) The expanding amyloid
624 family: Structure, stability, function, and pathogenesis. *Cell* 184: 4857-4873
625 Seki T, Kanagawa M, Kobayashi K, Kowa H, Yahata N, Maruyama K, Iwata N, Inoue H, Toda T
626 (2020) Galectin 3-binding protein suppresses amyloid-β production by modulating β-cleavage
627 of amyloid precursor protein. *J Biol Chem* 295: 3678-3691
628 Shinoda H, Ma Y, Nakashima R, Sakurai K, Matsuda T, Nagai T (2018) Acid-Tolerant
629 Monomeric GFP from Olindias formosa. *Cell Chem Biol* 25: 330-338.e337
630 Sipe JD, Benson MD, Buxbaum JN, Ikeda SI, Merlini G, Saraiva MJ, Westermark P (2016)
631 Amyloid fibril proteins and amyloidosis: chemical identification and clinical classification
632 International Society of Amyloidosis 2016 Nomenclature Guidelines. *Amyloid* 23: 209-213
633 Sun L, Ye RD (2016) Serum amyloid A1: Structure, function and gene polymorphism. *Gene* 583:
634 48-57
635 Toh K, Nishio K, Nakagawa R, Egoshi S, Abo M, Perron A, Sato SI, Okumura N, Koizumi N,
636 Dodo K *et al* (2022) Chemoproteomic Identification of Blue-Light-Damaged Proteins. *J Am*
637 *Chem Soc* 144: 20171-20176
638 Tomihari A, Chiba M, Matsuura A, Itakura E (2021) Protocol for quantification of the lysosomal
639 degradation of extracellular proteins into mammalian cells. *STAR Protoc* 2: 100975
640 Tomihari A, Kiyota M, Matsuura A, Itakura E (2023) Alpha 2-macroglobulin acts as a clearance
641 factor in the lysosomal degradation of extracellular misfolded proteins. *Sci Rep* 13: 4680
642 Tyedmers J, Mogk A, Bukau B (2010) Cellular strategies for controlling protein aggregation. *Nat*
643 *Rev Mol Cell Biol* 11: 777-788
644 Uhlar CM, Whitehead AS (1999) Serum amyloid A, the major vertebrate acute-phase reactant.
645 *Eur J Biochem* 265: 501-523
646 Westermark GT, Engström U, Westermark P (1992) The N-terminal segment of protein AA
647 determines its fibrillogenic property. *Biochem Biophys Res Commun* 182: 27-33

Wilson PG, Thompson JC, Shridas P, McNamara PJ, de Beer MC, de Beer FC, Webb NR, Tannock LR (2018) Serum Amyloid A Is an Exchangeable Apolipoprotein. *Arterioscler Thromb Vasc Biol* 38: 1890-1900

Wolff S, Weissman JS, Dillin A (2014) Differential scales of protein quality control. *Cell* 157: 52-64

Wyatt AR, Yerbury JJ, Ecroyd H, Wilson MR (2013) Extracellular chaperones and proteostasis. *Annu Rev Biochem* 82: 295-322

Xu D, Esko JD (2014) Demystifying heparan sulfate-protein interactions. *Annu Rev Biochem* 83: 129-157

Yayon A, Klagsbrun M, Esko JD, Leder P, Ornitz DM (1991) Cell surface, heparin-like molecules are required for binding of basic fibroblast growth factor to its high affinity receptor. *Cell* 64: 841-848

661 Figure 1. Identification of GPLD1 as an extracellular scavenger carrier
662 (**A**) Schematic of the RFP-GFP internalization assay. Upon internalization, the protein of interest (POI)
663 and GFP are degraded by lysosomal proteases, whereas RFP is resistant to lysosomal degradation and
664 accumulates in lysosomes. (**B**) RFP intensity increases when GPLD1-RFP-GFP is incubated with
665 SAA1. POI-RG with or without ALFA-SAA1-N in serum-free medium (advanced DMEM/F12) was
666 preincubated at 37°C with shaking for 2 h. HEK293 cells were treated with the medium for 18 h and
667 analyzed by flow cytometry. (**C**, **D**) GPLD1-RFP-GFP is degraded in lysosomes. GPLD1-RG with or
668 without ALFA-SAA1-N in serum-free medium was preincubated at 37°C with shaking for 2 h.
669 HEK293 cells were treated with the media in the presence or absence of bafilomycin A_1 (BafA) for 18
670 h. Cells were analyzed by flow cytometry (C) or immunoblotting using anti-mCherry and anti-β-
671 tubulin antibodies (D). The bar graph shows relative fluorescence intensities normalized to non-treated
672 cells (n = 3)(C). The relative band intensity is the -fold change of each sample's intensity, normalized
673 to the intensity of ALFA-SAA1-N treated cells, which was set to 1.0 (n = 3) (D). Data are presented
674 as mean ± SEM. Exact p-values are also shown above the bars.
675
676 Figure 2. GPLD1 directly interacts with aberrant proteins
677 (**A**) Recombinant GPLD1-RFP-GFP was mixed with or without ALFA-SAA1-N or -F in PBS and
678 preincubated at 37°C with shaking for 2 h. Samples were then subjected to immunoprecipitation using
679 ALFA-nanobody beads at 4°C. (**B**) Recombinant GPLD1-RFP-GFP was mixed with or without
680 luciferase in PBS and incubated at 42°C for 30 min. Samples were subjected to immunoprecipitation
681 using GFP nanobody beads at 4°C. The relative band intensity is the -fold change of each sample's
682 intensity, normalized to the intensity of SAA1-N or Luciferase at 42°C treated cells, which was set to
683 1.0 (n = 3). Data are presented as mean ± SEM. Exact p-values are also shown above the bars.
684
685
686 Figure 3. GPLD1 mediates lysosomal degradation of misfolded proteins
687 (**A**) GPLD1-RFP-GFP internalization is enhanced in the presence of misfolded proteins. GPLD1-RFP-
688 GFP was preincubated either alone (50°C for 1 h), with luciferase (Luc) (42°C for 30 min), or ALFA-
689 ESD (50°C for 1 h) in serum-free medium. HEK293 cells were cultured with medium containing
690 GPLD1-RFP-GFP with or without substrate for 18 h and analyzed by flow cytometry. (**B**) GPLD1 is
691 transported into lysosomes. GPLD1-Gamillus was preincubated with luciferase (42°C for 30 min) or
692 ALFA-SAA1-N (SAA1) (37°C with shaking for 2 h) in serum-free medium. HuEhT cells were treated
693 with the medium for 18 h. Cells were immunostained for LAMP1 (lysosomal marker) and imaged by
694 confocal microscopy. Scale bar, 10 μm. (**C**, **D**) GPLD1-RFP-GFP and substrate complexes are
695 degraded in lysosomes. HEK293 cells were treated as in (**A**) in the presence or absence of bafilomycin
696 A_1, then analyzed by flow cytometry (C) or immunoblotting with anti-mCherry, anti-luciferase, and
697 anti-β-tubulin antibodies (D). The bar graph shows relative fluorescence intensities per cell normalized
698 to untreated controls (n = 3) (A, C). The number of GPLD1 puncta co-localizing with Lamp1 per cell
699 is shown (n = 50) (B). The relative band intensity is the -fold change of each sample's intensity,
700 normalized to the intensity of luciferase treated cells, which was set to 1.0 (n = 3) (D). Data are
701 presented as mean ± SEM. Exact p-values are also shown above the bars.

Figure 4. GPLD1 internalization is independent of GPI-anchored protein cleavage

(**A**) Catalytic activity of GPLD1 is not required for its internalization. Wild-type (WT) GPLD1-RFP-GFP or catalytic mutants (H133N, H158N) were preincubated with luciferase (42°C for 30 min) or ALFA-SAA1-N (37°C with shaking for 2 h) in serum-free medium. HEK293 cells were treated with medium containing GPLD1-RFP-GFP with or without substrate for 18 h and analyzed by flow cytometry. (**B**) Confirmation of GPAA1 knockout (KO) by immunoblotting wild-type and GPAA1 KO HeLa cell lysates with anti-GPAA1 antibody. # indicates non-specific signals. (**C**) GPAA1 KO cells fail to mature GPI-anchored proteins. Wild-type and GPAA1 KO HeLa cells expressing GFP-GPI were analyzed by confocal microscopy. Scale bar, 10 μm. (**D**, **E**) GPLD1 internalization is not impaired in GPAA1 KO cells. Wild-type and GPAA1 KO HeLa cells were treated as in (A) and analyzed by flow cytometry (D) or immunoblotting with anti-mCherry and anti-β-tubulin antibodies (E). The bar graph shows relative fluorescence intensity per cell normalized to untreated controls (n = 3) (A, D). The relative band intensity is the -fold change of each sample's intensity, normalized to the intensity of luciferase treated cells, which was set to 1.0 (n = 3) (E). Data are presented as mean ± SEM. Exact p-values are also shown above the bars.

Figure 5. Internalization of GPLD1 depends on heparan sulfate (HS)

(**A**) GPLD1 directly binds HS. Recombinant GPLD1-RFP-GFP or RFP-GFP, in the presence or absence of free heparin, was subjected to a pulldown assay using heparin-conjugated beads. The relative band intensity of GPLD1-RG is the -fold change of each sample's intensity (n = 3) (**B**) EXT1 KO cells show reduced GPLD1-RFP-GFP internalization. GPLD1-RFP-GFP was preincubated with luciferase (42°C for 30 min) in serum-free medium. HEK293 wild-type (WT), EXT1 KO cells complemented with EXT1 (overexpression, OE), or empty vector were cultured in medium containing GPLD1-RFP-GFP with or without luciferase for 18 h and analyzed by flow cytometry. The bar graph shows relative fluorescence intensity per cell normalized to untreated cells (n = 3). Data are presented as mean ± SEM. Exact p-values and effect sizes (Cohen's d) are also shown above the bars. (**C**) Excess free heparin inhibits GPLD1-RFP-GFP internalization. GPLD1-RFP-GFP was incubated with luciferase (42°C for 30 min) or ALFA-SAA1-N (37°C with shaking for 2 h) in serum-free medium. HEK293 cells (for ALFA-SAA1-N) or HuEhT cells (for luciferase) were treated with medium containing GPLD1-RFP-GFP in the presence or absence of heparin for 18 h and analyzed by flow cytometry. The bar graph shows relative fluorescence intensity per cell normalized to the non-heparin treated control (n = 3). Data are presented as mean ± SEM. Exact p-values and effect sizes (Cohen's d) are also shown above the bars.

Figure 6. GPLD1 and clusterin exhibit different specificities

(**A**) GPLD1, but not clusterin, shows higher specificity for SAA1. GPLD1-RFP-GFP (0.2 μM) or clusterin-RFP-GFP (0.2 μM) was incubated with 0.2 μM luciferase (42°C for 30 min), 8 μM ALFA-SAA1-N (37°C with shaking for 2 h), or 8 μM amyloid β1-42 (Ab42) (37°C with shaking for 2 h) in serum-free medium. HuEhT cells were treated with the medium containing GPLD1-RFP-GFP or clusterin-RFP-GFP, with or without substrate, for 18 h and analyzed by flow cytometry. The bar graph

743 shows relative fluorescence intensity per cell normalized to non-treated controls (n = 3). (**B**)
744 Differential substrate preferences of GPLD1 and Clusterin. Recombinant GPLD1-RFP-GFP or
745 Clusterin-RFP-GFP was mixed with or without Luc, ALFA-SAA1-N, or ALFA-Ab42 in PBS and
746 preincubated at 37°C with shaking for 2 h. Samples were then subjected to immunoprecipitation using
747 ALFA-nanobody beads at 4°C. The relative band intensity is the -fold change of each sample's
748 intensity, normalized to the intensity of Clusterin-RG with Ab42-ALFA or GPLD1-RG with ALFA-
749 SAA1-N, which was set to 1.0. Data are presented as mean ± SEM. Exact p-values are also shown
750 above the bars (n = 3). Data are presented as mean ± SEM. Exact p-values and effect sizes (extn's d)
751 are also shown above the bars. (**C**) Model of the extracellular aberrant protein degradation pathway
752 by GPLD1. GPLD1 interacts with misfolded proteins and SAA1, and the GPLD1 complex is delivered
753 to lysosomes via cell surface heparan sulfate.
754
755 Figure S1 Plasma proteins interact with SAA1.
756 (**A**) SAA1-N is aggregated in PBS. Urea-denatured ALFA-SAA1-N (final 8 μM) or albumin-ALFA
757 (final 2 μM) was incubated (37°C, 2 h, shaking) in PBS or internalization assay medium (AdDMEM).
758 Supernatant (Sup) and pellet (Pel) fractions were separated by centrifugation and subjected to
759 immunoblotting using an anti-SAA1 and anti-ALFA antibodies. While denatured ALFA-SAA1-N
760 predominantly partitions into the pellet fraction in PBS, it remains entirely in the soluble fraction when
761 incubated in Advanced DMEM/F12. This enhanced solubility is likely mediated by the chaperone-like
762 effect of the supplemental albumin in the medium, ensuring that SAA1-N is not lost during the
763 centrifugal steps of the internalization assay. The relative band intensity is the -fold change of each
764 sample's intensity, normalized to the intensity of Total, which was set to 1.0 (n = 3). (**B**) Bovine plasma
765 was mixed with recombinant ALFA-SAA1-N, co-immunoprecipitated with ALFA nanobody beads,
766 and analyzed by Ruby staining. Arrowheads indicate SAA1-binding proteins. (C) SAA1-concentration
767 dependent internalization of GPLD1-RFP-GFP. 0.2 μM GPLD1-RG was preincubated in serum-free
768 medium at 37°C for 2 h with shaking, either alone or in the presence of urea-denatured 2-8 μM SAA1-
769 N. After incubation, the medium was added to HEK293 cells for 18 h, followed by flow cytometric
770 analysis. The bar graph shows relative fluorescence intensities per cell normalized to untreated
771 controls (n = 3). Data are presented as mean ± SEM. Exact p-values are also shown above the bars.
772
773
774 Figure S2 Protein substrate-specific internalization of GPLD1.
775 (**A**) Urea alone is insufficient to trigger GPLD1-RG internalization. GPLD1-RG with or without 50
776 mM urea in serum-free medium was preincubated at 37°C with shaking for 2 h. HEK293 cells were
777 cultured with the medium for 18 h and analyzed by flow cytometry. Internalization of GPLD1-RG was
778 not dependent of 50 mM urea and heat stress. (**B**) Bafilomycin A_1 (BafA) impairs endocytosis of
779 albumin. HEK293 cells were cultured with medium containing albumin-565 in the presence or absence
780 of BafA for 18 h and analyzed by flow cytometry. Internalization of albumin is inhibited by treatment
781 of BafA, indicating that BafA suppresses not only lysosomal proteases, but also endocytosis. (**C**)
782 GPLD1 might recognize aggregated substrates. GPLD1-RG, ALFA-SAA1-N, or a mixture of both in
783 serum-free medium was preincubated at 37°C with shaking for 2 h. HEK293 cells were cultured with

784 the media for 18 h and analyzed by flow cytometry. The bar graph shows relative fluorescence
785 intensities per cell normalized to untreated controls (n = 3; A and C), (n = 6; B). Data are presented as
786 mean ± SEM. Exact p-values are also shown above the bars.
787
788 Figure S3 SAA1-N, but not SAA1-F, is aggregated.
789 (**A**) SAA1-full-length (SAA1-F) does not promote internalization of GPLD1. 0.2 μM GPLD1-RG was
790 preincubated in serum-free medium at 37°C for 2 h with shaking, either alone or in the presence of
791 urea-denatured 8 μM SAA1-N, urea-denatured 8 μM SAA1-F, or native 8 μM SAA1-F. After
792 incubation, the medium was added to HEK293 cells for 18 h, followed by flow cytometric analysis.
793 The bar graph shows relative fluorescence intensities per cell normalized to untreated controls (n = 5).
794 (**B**) SAA1-F is not aggregated in PBS. Urea-denatured ALFA-SAA1-F, or native ALFA-SAA1-F
795 (Final 8 μM) in PBS was incubated at 37°C for 2 h with shaking. After centrifugation, supernatant
796 (Sup) and pellet (Pel) fractions were analyzed by immunoblotting using anti-SAA1 antibody. (**C**)
797 GPLD1 does not prevent formation of SAA1-aggregates. Urea-denatured ALFA-SAA1 (Final 2 μM)
798 in PBS was incubated at 37°C for 2 h with shaking, either alone or in the presence of 2 μM GPLD1-
799 RG, or 2 μM Albumin-ALFA. After centrifugation, Sup and Pel fractions were analyzed by
800 immunoblotting using anti-SAA1 antibody. The relative band intensity is the -fold change of each
801 sample's intensity, normalized to the intensity of Total, which was set to 1.0 (n = 3) (B and C). Data
802 are presented as mean ± SEM. Exact p-values are also shown above the bars.
803
804 Figure S4. Heat stress alone does not affect the internalization of GPLD1-RG.
805 (**A**) Heat stress alone is insufficient to trigger GPLD1-RG internalization. GPLD1-RG in serum-free
806 medium was preincubated at 42°C or 50°C for 1 h. HEK293 cells were cultured with the medium for
807 18 h and analyzed by flow cytometry. The bar graph shows relative fluorescence intensities per cell
808 normalized to untreated controls (n = 3). (**B**) GPLD1 does not co-precipitate with protein aggregates.
809 0.2 μM GPLD1-RG was incubated in serum-free medium either alone or in the presence of the
810 following proteins to induce aggregation: luciferase (0.2 μM, 42°C, 0.5 h), urea-denatured SAA1-N
811 (8 μM; 37°C, 2 h with shaking), native SAA1-F (8 μM; 37°C, 2 h with shaking), or ALFA-ESD (8
812 μM; 50°C, 1 h) (under the same conditions as the internalization assay). After centrifugation, Sup and
813 Pel fractions were analyzed by immunoblotting using anti-GFP antibody. (**C**) GPLD1 does not form
814 aggregates by heat stress. 0.2 μM GPLD1-RG in PBS or internalization assay medium (AdDMEM)
815 was incubated at 50°C for 1 h. After centrifugation, Sup and Pel fractions were analyzed by
816 immunoblotting using anti-GFP antibody. The relative band intensity is the -fold change of each
817 sample's intensity, normalized to the intensity of Total, which was set to 1.0 (n = 3) (B and C). Data
818 are presented as mean ± SEM. Exact p-values are also shown above the bars.
819
820
821 Figure S5. GPLD1-substrate complex is internalized in various cell lines
822 HuEhT, U2OS, T98G, and HepG2 were treated with medium containing GPLD1-RFP-GFP as
823 described in Figs. 1B and 3A and analyzed by flow cytometry. The bar graph shows relative
824 fluorescence intensities per cell normalized to untreated controls (n = 3). Data are presented as mean

825 ± SEM. Exact p-values are also shown above the bars.
826
827 Figure S6. Expression level of GPLD1-RFP-GFP wild-type, H133N, and H158N
828 HEK293 cells stably expressing the indicated GPLD1-RG (wild-type, H133N, or H158N) were
829 cultured for 4 days in serum-free Advanced DMEM/F12 medium supplemented with doxycycline. The
830 conditioned media were analyzed by immunoblotting using an anti-GFP antibody. The observation
831 that the GPLD1 catalytic mutants were secreted at levels comparable to the wild type suggests that
832 their folding within the endoplasmic reticulum (ER) was not impaired. The relative band intensity is
833 the -fold change of each sample's intensity, normalized to the intensity of wild-type, which was set to
834 1.0 (n = 3). Data are presented as mean ± SEM. Exact p-values are also shown above the bars.
835
836 Table S1. List of proteins identified by mass spectrometry.
837 The table shows the total spectral counts and the ratio of SAA1-N to the control.
838
839 Table S2. Raw fluorescence intensity values from flow cytometry analysis.
840 Raw mean fluorescence intensity (MFI) values are listed for each GFP and RFP across all biological
841 replicates.

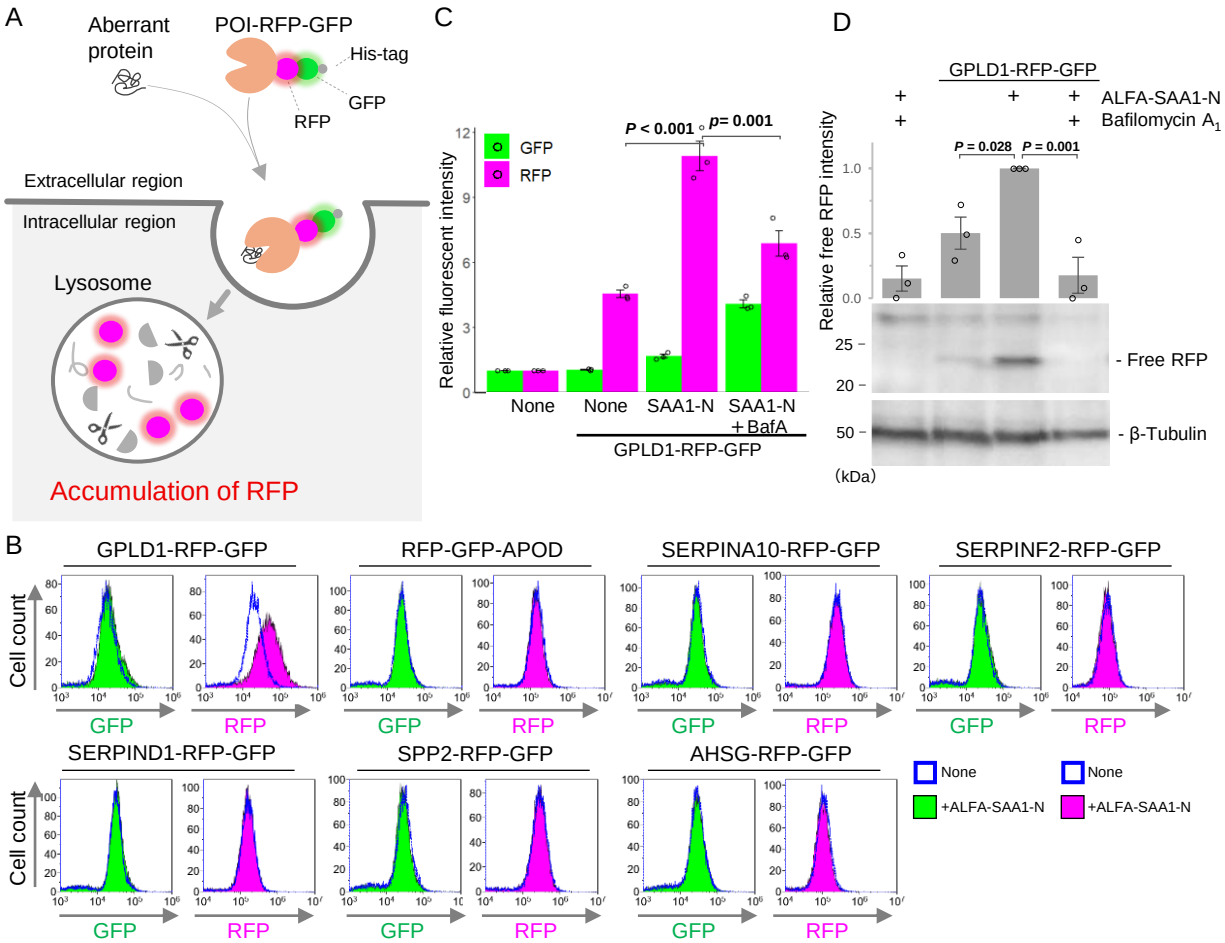

Figure 1. Identification of GPLD1 as an extracellular scavenger carrier

(**A**) Schematic of the RFP-GFP internalization assay. Upon internalization, the protein of interest (POI) and GFP are degraded by lysosomal proteases, whereas RFP is resistant to lysosomal degradation and accumulates in lysosomes. (**B**) RFP intensity increases when GPLD1-RFP-GFP is incubated with SAA1. POI-RG with or without ALFA-SAA1-N in serum-free medium (advanced DMEM/F12) was preincubated at 37° C with shaking for 2 h. HEK293 cells were treated with the medium for 18 h and analyzed by flow cytometry. (**C**, **D**) GPLD1-RFP-GFP is degraded in lysosomes. GPLD1-RG with or without ALFA-SAA1-N in serum-free medium was preincubated at 37° C with shaking for 2 h. HEK293 cells were treated with the media in the presence or absence of bafilomycin A_1 (BafA) for 18 h. Cells were analyzed by flow cytometry (C) or immunoblotting using anti-mCherry and anti-β-tubulin antibodies (D). The bar graph shows relative fluorescence intensities normalized to non-treated cells (n = 3)(C). The relative band intensity is the -fold change of each sample's intensity, normalized to the intensity of ALFA-SAA1-N treated cells, which was set to 1.0 (n = 3) (D). Data are presented as mean ± SEM. Exact p-values are also shown above the bars.

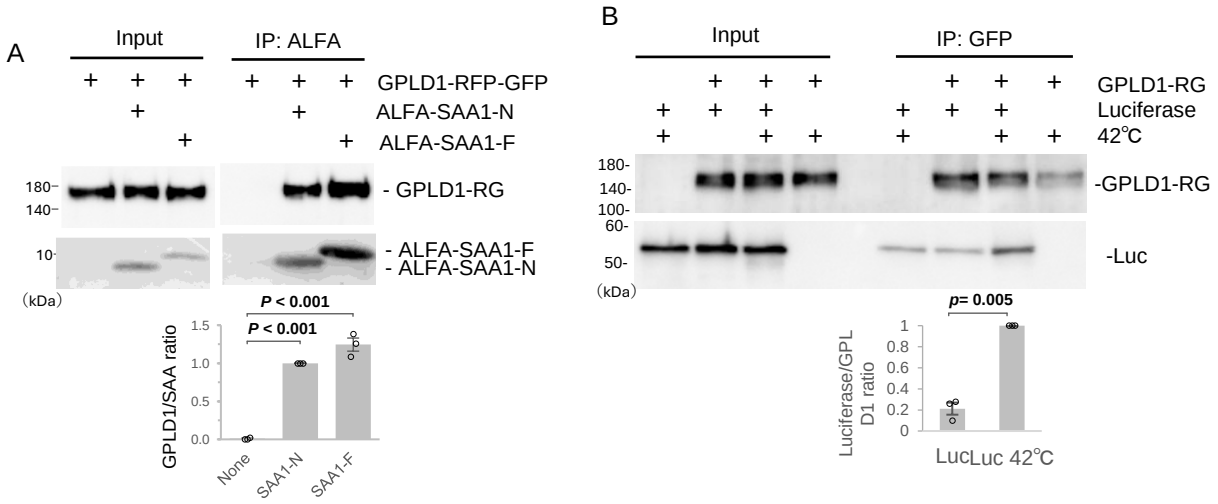

Figure 2. GPLD1 directly interacts with aberrant proteins

(**A**) Recombinant GPLD1-RFP-GFP was mixed with or without ALFA-SAA1-N or -F in PBS and preincubated at 37° C with shaking for 2 h. Samples were then subjected to immunoprecipitation using ALFA-nanobody beads at 4° C. (**B**) Recombinant GPLD1-RFP-GFP was mixed with or without luciferase in PBS and incubated at 42° C for 30 min. Samples were subjected to immunoprecipitation using GFP nanobody beads at 4° C. The relative band intensity is the -fold change of each sample's intensity, normalized to the intensity of SAA1-N or Luciferase at 42° C treated cells, which was set to 1.0 (n = 3). Data are presented as mean ± SEM. Exact p-values are also shown above the bars.

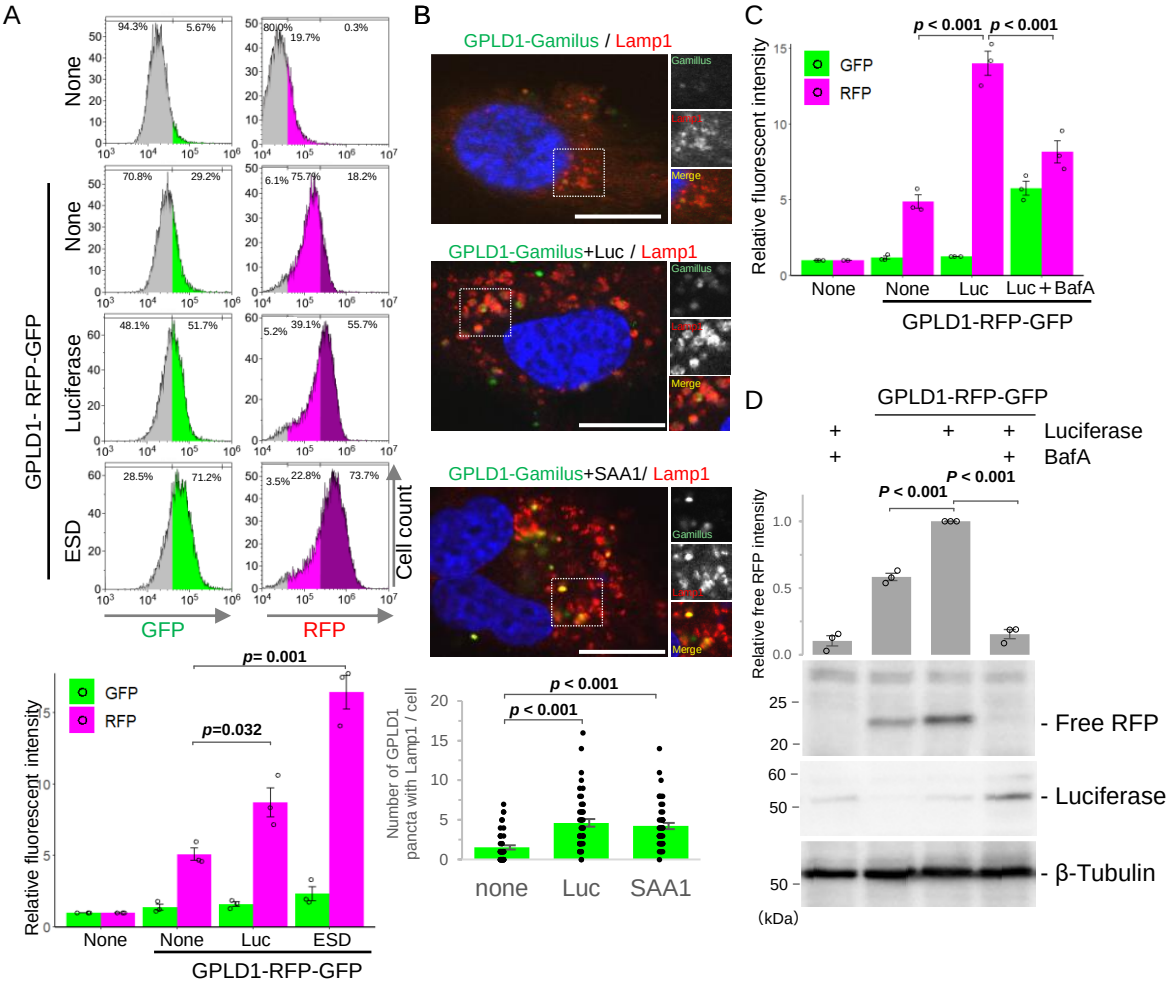

Figure 3. GPLD1 mediates lysosomal degradation of misfolded proteins

(**A**) GPLD1-RFP-GFP internalization is enhanced in the presence of misfolded proteins. GPLD1-RFP-GFP was preincubated either alone (50° C for 1 h), with luciferase (Luc) (42° C for 30 min), or ALFA-ESD (50° C for 1 h) in serum-free medium. HEK293 cells were cultured with medium containing GPLD1-RFP-GFP with or without substrate for 18 h and analyzed by flow cytometry. (**B**) GPLD1 is transported into lysosomes. GPLD1-Gamillus was preincubated with luciferase (42° C for 30 min) or ALFA-SAA1-N (SAA1) (37° C with shaking for 2 h) in serum-free medium. HuEhT cells were treated with the medium for 18 h. Cells were immunostained for LAMP1 (lysosomal marker) and imaged by confocal microscopy. Scale bar, 10 µm. (**C**, **D**) GPLD1-RFP-GFP and substrate complexes are degraded in lysosomes. HEK293 cells were treated as in (**A**) in the presence or absence of bafilomycin A_1, then analyzed by flow cytometry (C) or immunoblotting with anti-mCherry, anti-luciferase, and anti-β-tubulin antibodies (D). The bar graph shows relative fluorescence intensities per cell normalized to untreated controls (n = 3) (A, C). The number of GPLD1 puncta co-localizing with Lamp1 per cell is shown (n = 50) (B). The relative band intensity is the -fold change of each sample's intensity, normalized to the intensity of luciferase treated cells, which was set to 1.0 (n = 3) (D). Data are presented as mean ± SEM. Exact p-values are also shown above the bars.

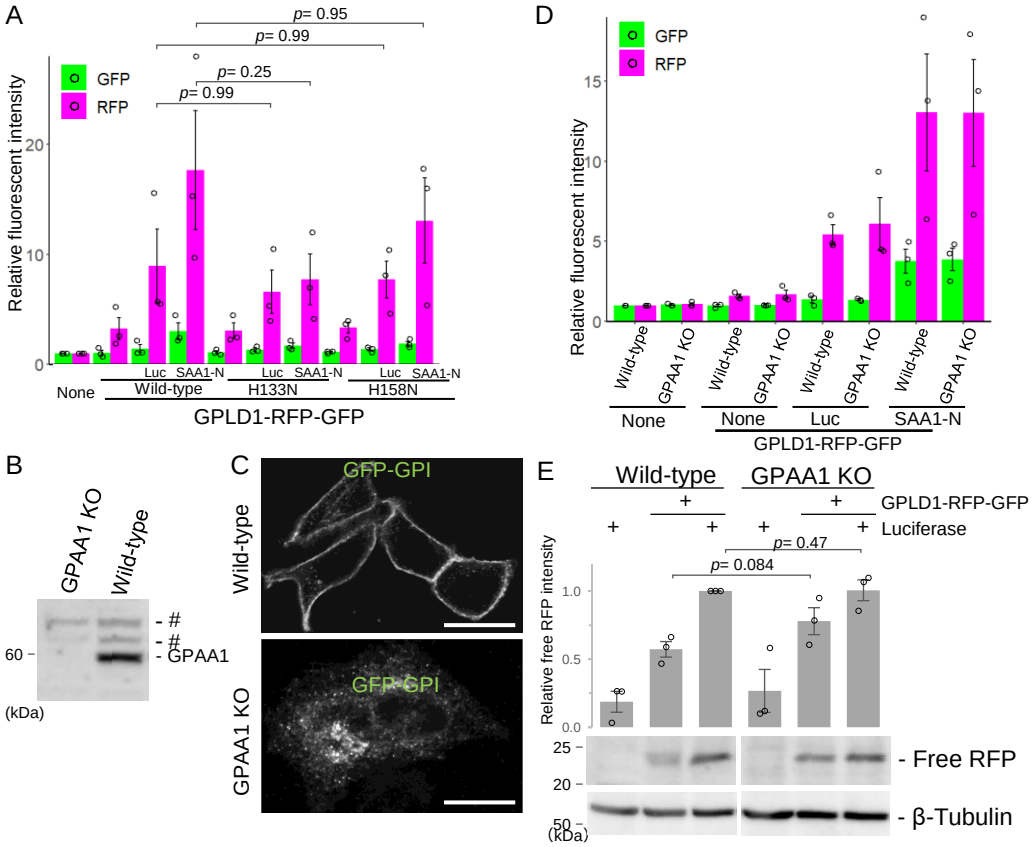

Figure 4. GPLD1 internalization is independent of GPI-anchored protein cleavage

(**A**) Catalytic activity of GPLD1 is not required for its internalization. Wild-type (WT) GPLD1-RFP-GFP or catalytic mutants (H133N, H158N) were preincubated with luciferase (42° C for 30 min) or ALFA-SAA1-N (37° C with shaking for 2 h) in serum-free medium. HEK293 cells were treated with medium containing GPLD1-RFP-GFP with or without substrate for 18 h and analyzed by flow cytometry. (**B**) Confirmation of GPAA1 knockout (KO) by immunoblotting wild-type and GPAA1 KO HeLa cell lysates with anti-GPAA1 antibody. # indicates non-specific signals. (**C**) GPAA1 KO cells fail to mature GPI-anchored proteins. Wild-type and GPAA1 KO HeLa cells expressing GFP-GPI were analyzed by confocal microscopy. Scale bar, 10 µm. (**D**, **E**) GPLD1 internalization is not impaired in GPAA1 KO cells. Wild-type and GPAA1 KO HeLa cells were treated as in (A) and analyzed by flow cytometry (D) or immunoblotting with anti-mCherry and anti-β-tubulin antibodies (E). The bar graph shows relative fluorescence intensity per cell normalized to untreated controls (n = 3) (A, D). The relative band intensity is the -fold change of each sample's intensity, normalized to the intensity of luciferase treated cells, which was set to 1.0 (n = 3) (E). Data are presented as mean ± SEM. Exact p-values are also shown above the bars.

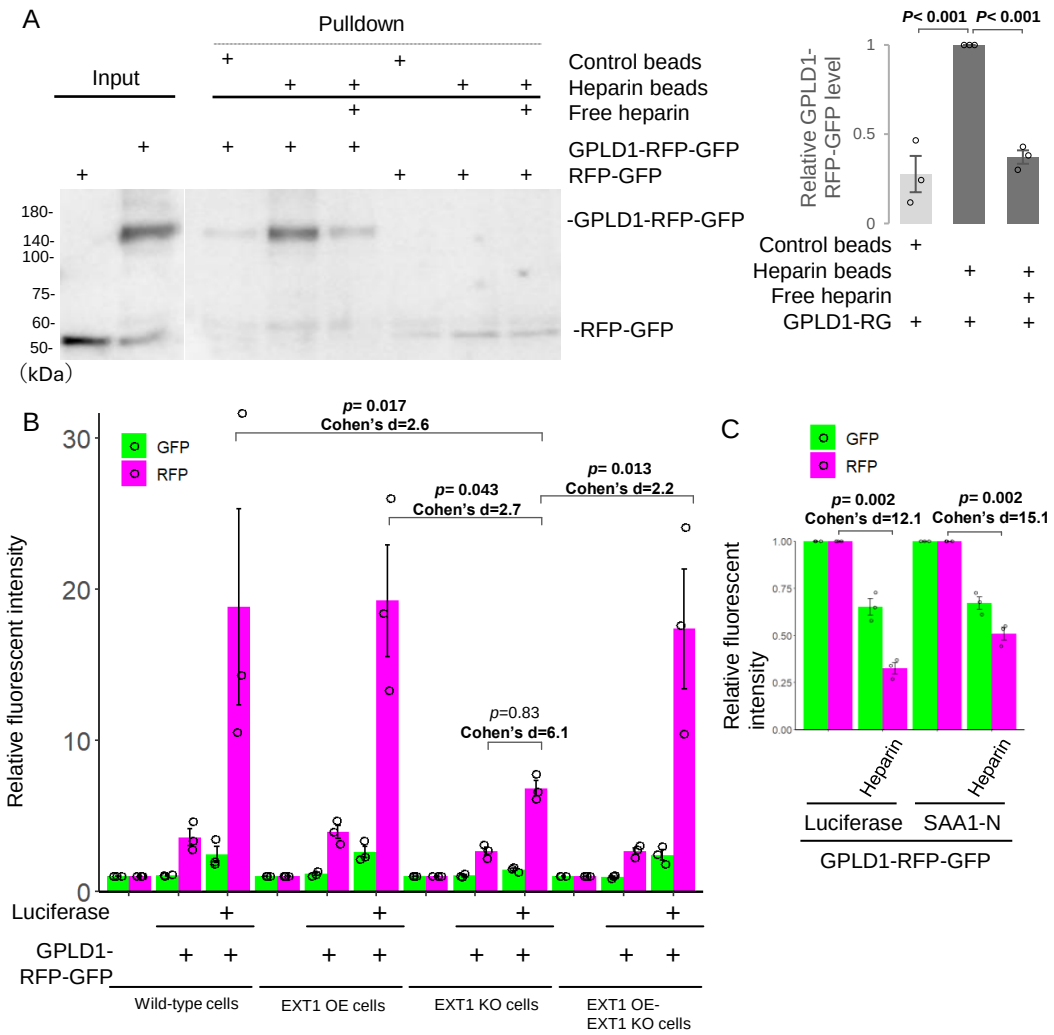

Figure 5. Internalization of GPLD1 depends on heparan sulfate (HS)

(**A**) GPLD1 directly binds HS. Recombinant GPLD1-RFP-GFP or RFP-GFP, in the presence or absence of free heparin, was subjected to a pulldown assay using heparin-conjugated beads. The relative band intensity of GPLD1-RG is the -fold change of each sample's intensity (n = 3) (**B**) EXT1 KO cells show reduced GPLD1-RFP-GFP internalization. GPLD1-RFP-GFP was preincubated with luciferase (42° C for 30 min) in serum-free medium. HEK293 wild-type (WT), EXT1 KO cells complemented with EXT1 (overexpression, OE), or empty vector were cultured in medium containing GPLD1-RFP-GFP with or without luciferase for 18 h and analyzed by flow cytometry. The bar graph shows relative fluorescence intensity per cell normalized to untreated cells (n = 3). Data are presented as mean ± SEM. Exact p-values and effect sizes (Cohen's d) are also shown above the bars. (**C**) Excess free heparin inhibits GPLD1-RFP-GFP internalization. GPLD1-RFP-GFP was incubated with luciferase (42° C for 30 min) or ALFA-SAA1-N (37° C with shaking for 2 h) in serum-free medium. HEK293 cells (for ALFA-SAA1-N) or HuEhT cells (for luciferase) were treated with medium containing GPLD1-RFP-GFP in the presence or absence of heparin for 18 h and analyzed by flow cytometry. The bar graph shows relative fluorescence intensity per cell normalized to the non-heparin treated control (n = 3). Data are presented as mean ± SEM. Exact p-values and effect sizes (Cohen's d) are also shown above the bars.

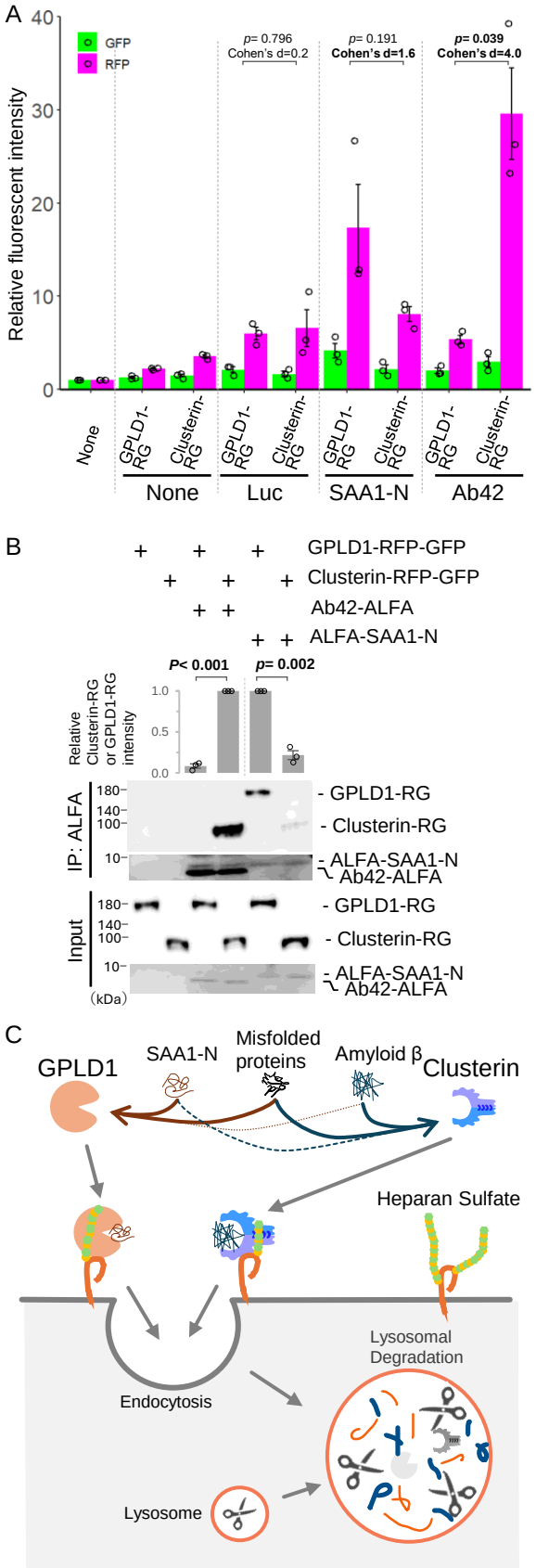

Figure 6. GPLD1 and clusterin exhibit different specificities (**A**) GPLD1, but not clusterin, shows higher specificity for SAA1. GPLD1-RFP-GFP (0.2 μM) or clusterin-RFP-GFP (0.2 μM) was incubated with 0.2 μM luciferase (42° C for 30 min), 8 μM ALFA-SAA1-N (37° C with shaking for 2 h), or 8 μM amyloid β1-42 (Ab42) (37° C with shaking for 2 h) in serum-free medium. HuEhT cells were treated with the medium containing GPLD1-RFP-GFP or clusterin-RFP-GFP, with or without substrate, for 18 h and analyzed by flow cytometry. The bar graph shows relative fluorescence intensity per cell normalized to non-treated controls (n = 3). (**B**) Differential substrate preferences of GPLD1 and Clusterin. Recombinant GPLD1-RFP-GFP or Clusterin-RFP-GFP was mixed with or without Luc, ALFA-SAA1-N, or ALFA-Ab42 in PBS and preincubated at 37° C with shaking for 2 h. Samples were then subjected to immunoprecipitation using ALFA-nanobody beads at 4° C. The relative band intensity is the -fold change of each sample's intensity, normalized to the intensity of Clusterin-RG with Ab42-ALFA or GPLD1-RG with ALFA-SAA1-N, which was set to 1.0. Data are presented as mean ± SEM. Exact p-values are also shown above the bars (n = 3). Data are presented as mean ± SEM. Exact p-values and effect sizes (extn's d) are also shown above the bars. (**C**) Model of the extracellular aberrant protein degradation pathway by GPLD1. GPLD1 interacts with misfolded proteins and SAA1, and the GPLD1 complex is delivered to lysosomes via cell surface heparan sulfate.

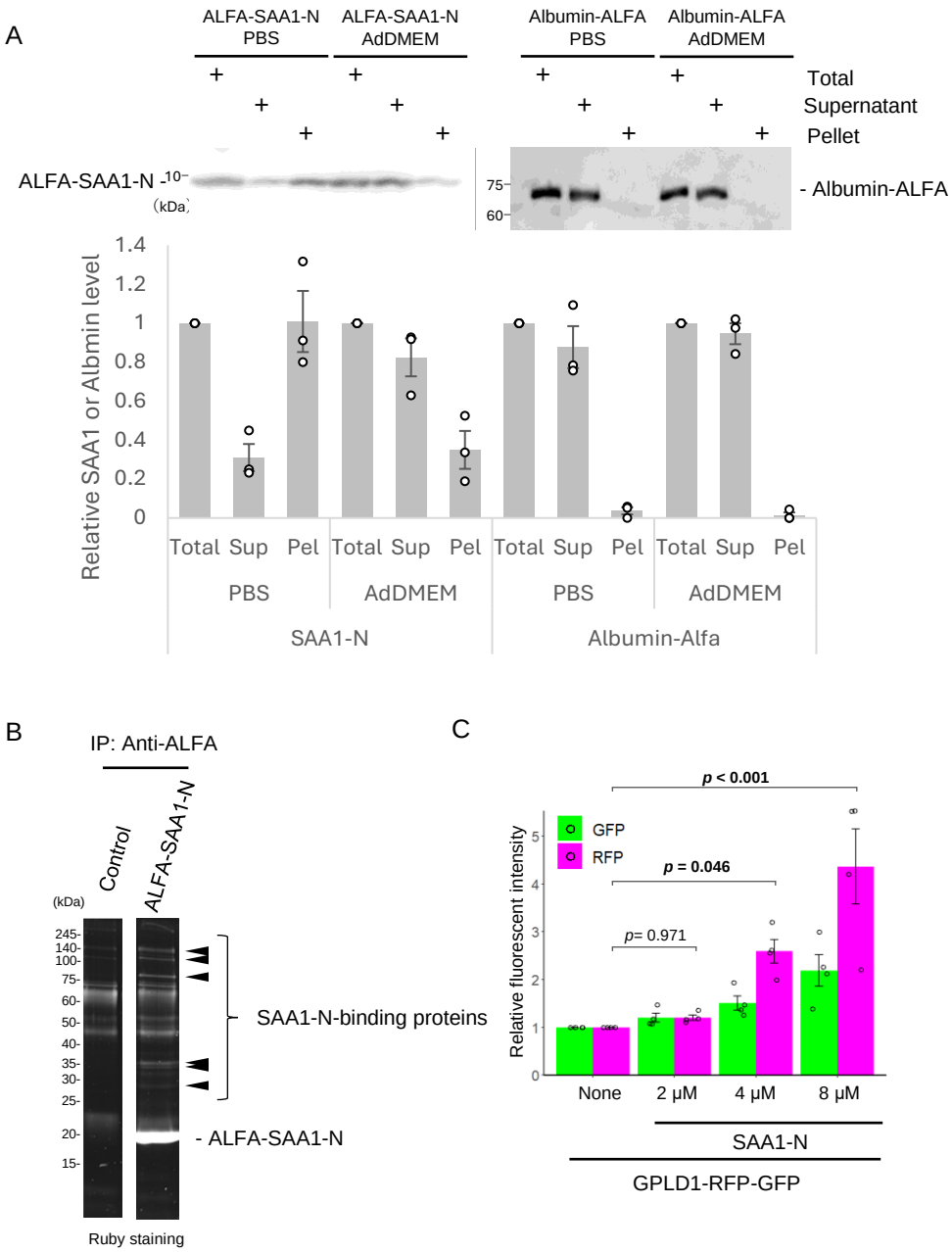

Figure S1 Plasma proteins interact with SAA1.

(**A**) SAA1-N is aggregated in PBS. Urea-denatured ALFA-SAA1-N (final 8 μM) or albumin-ALFA (final 2 μM) was incubated (37° C, 2 h, shaking) in PBS or internalization assay medium (AdDMEM). Supernatant (Sup) and pellet (Pel) fractions were separated by centrifugation and subjected to immunoblotting using an anti-SAA1 and anti-ALFA antibodies. While denatured ALFA-SAA1-N predominantly partitions into the pellet fraction in PBS, it remains entirely in the soluble fraction when incubated in Advanced DMEM/F12. This enhanced solubility is likely mediated by the chaperone-like effect of the supplemental albumin in the medium, ensuring that SAA1-N is not lost during the centrifugal steps of the internalization assay. The relative band intensity is the -fold change of each sample's intensity, normalized to the intensity of Total, which was set to 1.0 (n = 3). (**B**) Bovine plasma was mixed with recombinant ALFA-SAA1-N, co-immunoprecipitated with ALFA nanobody beads, and analyzed by Ruby staining. Arrowheads indicate SAA1-binding proteins. (C) SAA1-concentration dependent internalization of GPLD1-RFP-GFP. 0.2 μM GPLD1-RG was preincubated in serum-free medium at 37° C for 2 h with shaking, either alone or in the presence of urea-denatured 2-8 μM SAA1-N. After incubation, the medium was added to HEK293 cells for 18 h, followed by flow cytometric analysis. The bar graph shows relative fluorescence intensities per cell normalized to untreated controls (n = 3). Data are presented as mean ± SEM. Exact p-values are also shown above the bars.

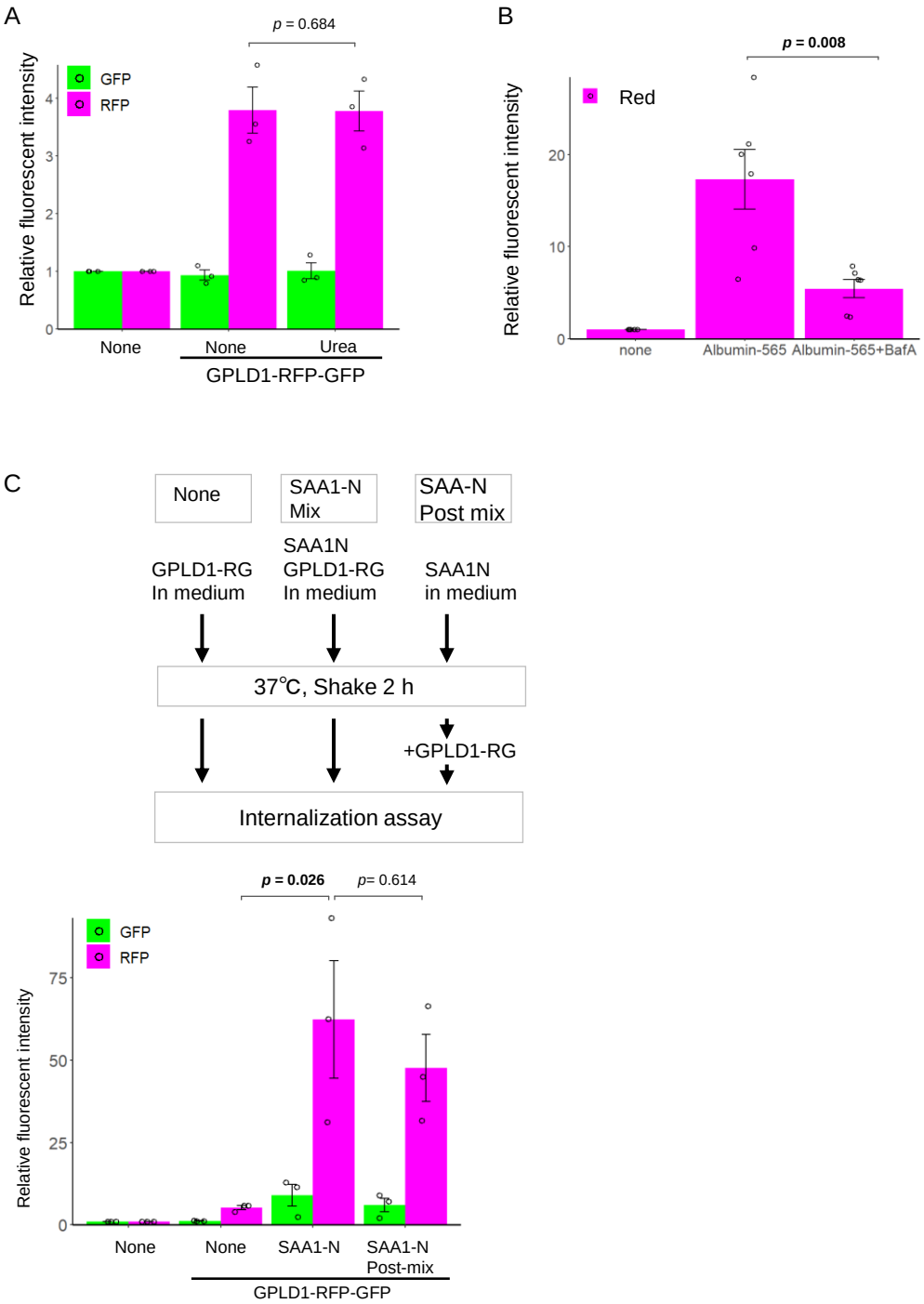

Figure S2 Protein substrate-specific internalization of GPLD1.

(**A**) Urea alone is insufficient to trigger GPLD1-RG internalization. GPLD1-RG with or without 50 mM urea in serum-free medium was preincubated at 37° C with shaking for 2 h. HEK293 cells were cultured with the medium for 18 h and analyzed by flow cytometry. Internalization of GPLD1-RG was not dependent of 50 mM urea and heat stress. (**B**) Bafilomycin A_1 (BafA) impairs endocytosis of albumin. HEK293 cells were cultured with medium containing albumin-565 in the presence or absence of BafA for 18 h and analyzed by flow cytometry. Internalization of albumin is inhibited by treatment of BafA, indicating that BafA suppresses not only lysosomal proteases, but also endocytosis. (**C**) GPLD1 might recognize aggregated substrates. GPLD1-RG, ALFA-SAA1-N, or a mixture of both in serum-free medium was preincubated at 37° C with shaking for 2 h. HEK293 cells were cultured with the media for 18 h and analyzed by flow cytometry. The bar graph shows relative fluorescence intensities per cell normalized to untreated controls (n = 3; A and C), (n = 6; B). Data are presented as mean ± SEM. Exact p-values are also shown above the bars.

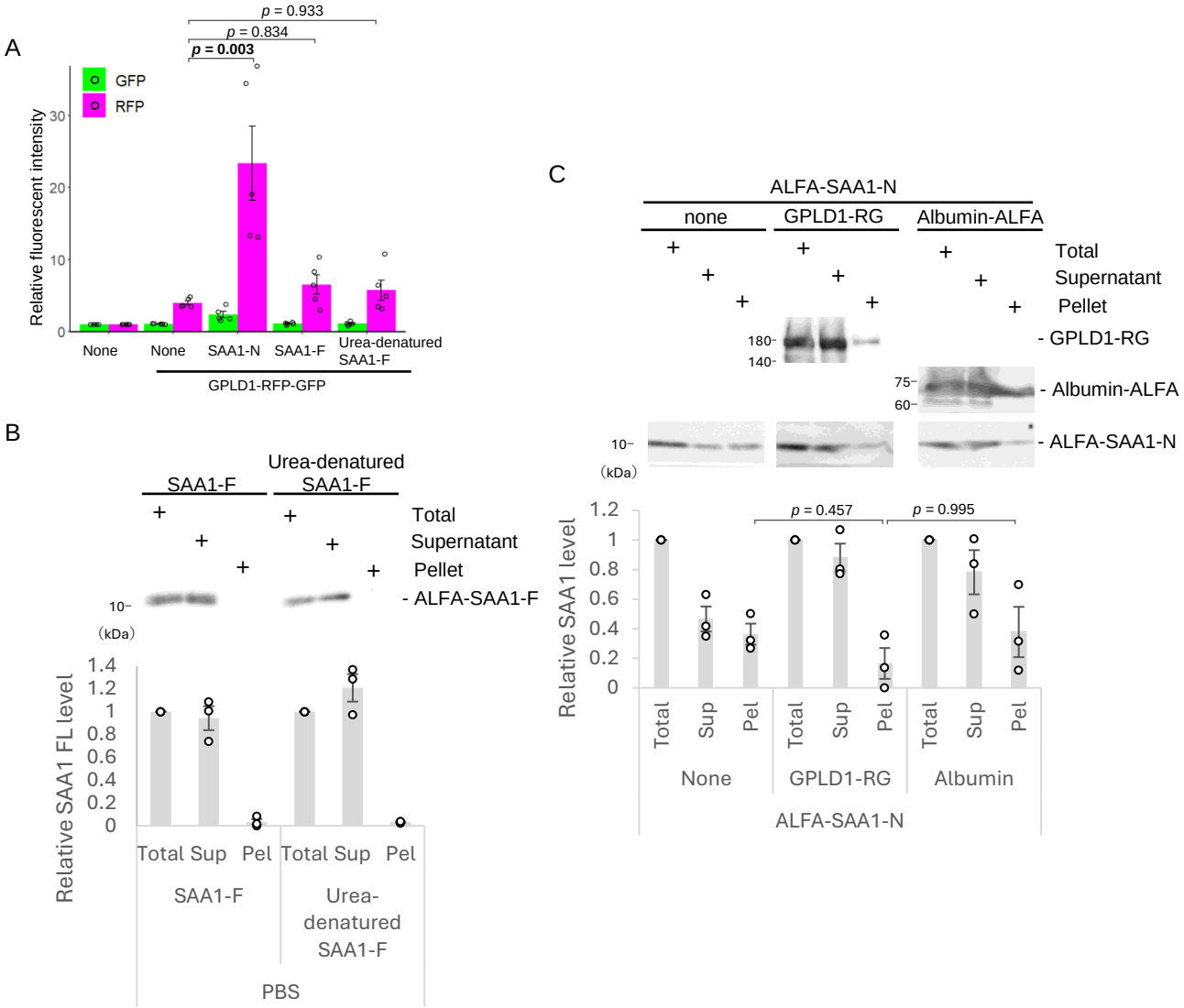

Figure S3 SAA1-N, but not SAA1-F, is aggregated.

(**A**) SAA1-full-length (SAA1-F) does not promote internalization of GPLD1. 0.2 μM GPLD1-RG was preincubated in serum-free medium at 37° C for 2 h with shaking, either alone or in the presence of urea-denatured 8 μM SAA1-N, urea-denatured 8 μM SAA1-F, or native 8 μM SAA1-F. After incubation, the medium was added to HEK293 cells for 18 h, followed by flow cytometric analysis. The bar graph shows relative fluorescence intensities per cell normalized to untreated controls (n = 5). (**B**) SAA1-F is not aggregated in PBS. Urea-denatured ALFA-SAA1-N, urea-denatured ALFA-SAA1-F, or native ALFA-SAA1-F (Final 8 μM) in PBS was incubated at 37° C for 2 h with shaking. After centrifugation, supernatant (Sup) and pellet (Pel) fractions were analyzed by immunoblotting using anti-SAA1 antibody. (**C**) GPLD1 does not prevent formation of SAA1-aggregates. Urea-denatured ALFA-SAA1 (Final 2 μM) in PBS was incubated at 37° C for 2 h with shaking, either alone or in the presence of 2 μM GPLD1-RG, or 2 μM Albumin-ALFA. After centrifugation, Sup and Pel fractions were analyzed by immunoblotting using anti-SAA1 antibody. The relative band intensity is the -fold change of each sample's intensity, normalized to the intensity of Total, which was set to 1.0 (n = 3) (B and C). Data are presented as mean ± SEM. Exact p-values are also shown above the bars.

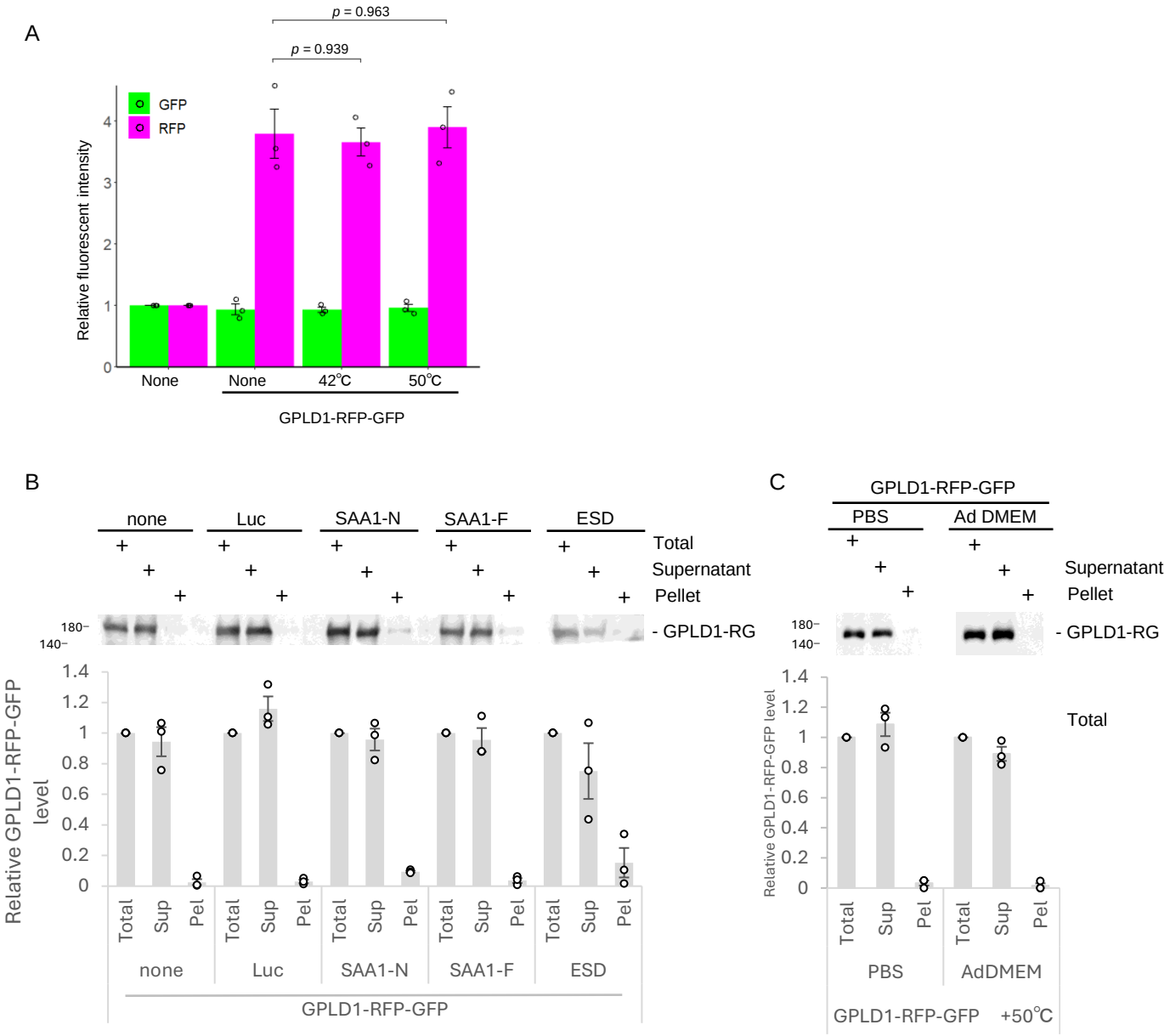

Figure S4. Heat stress alone does not affect the internalization of GPLD1-RG.

(**A**) Heat stress alone is insufficient to trigger GPLD1-RG internalization. GPLD1-RG in serum-free medium was preincubated at 42° C or 50° C for 1 h. HEK293 cells were cultured with the medium for 18 h and analyzed by flow cytometry. The bar graph shows relative fluorescence intensities per cell normalized to untreated controls (n = 3). (**B**) GPLD1 does not co-precipitate with protein aggregates. 0.2 μM GPLD1-RG was incubated in serum-free medium either alone or in the presence of the following proteins to induce aggregation: luciferase (0.2 μM, 42° C, 0.5 h), urea-denatured SAA1-N (8 μM; 37° C, 2 h with shaking), native SAA1-F (8 μM; 37° C, 2 h with shaking), or ALFA-ESD (8 μM; 50° C, 1 h) (under the same conditions as the internalization assay). After centrifugation, Sup and Pel fractions were analyzed by immunoblotting using anti-GFP antibody. (**C**) GPLD1 does not form aggregates by heat stress. 0.2 μM GPLD1-RG in PBS or internalization assay medium (AdDMEM) was incubated at 50° C for 1 h. After centrifugation, Sup and Pel fractions were analyzed by immunoblotting using anti-GFP antibody. The relative band intensity is the -fold change of each sample's intensity, normalized to the intensity of Total, which was set to 1.0 (n = 3) (B and C). Data are presented as mean ± SEM. Exact p-values are also shown above the bars.

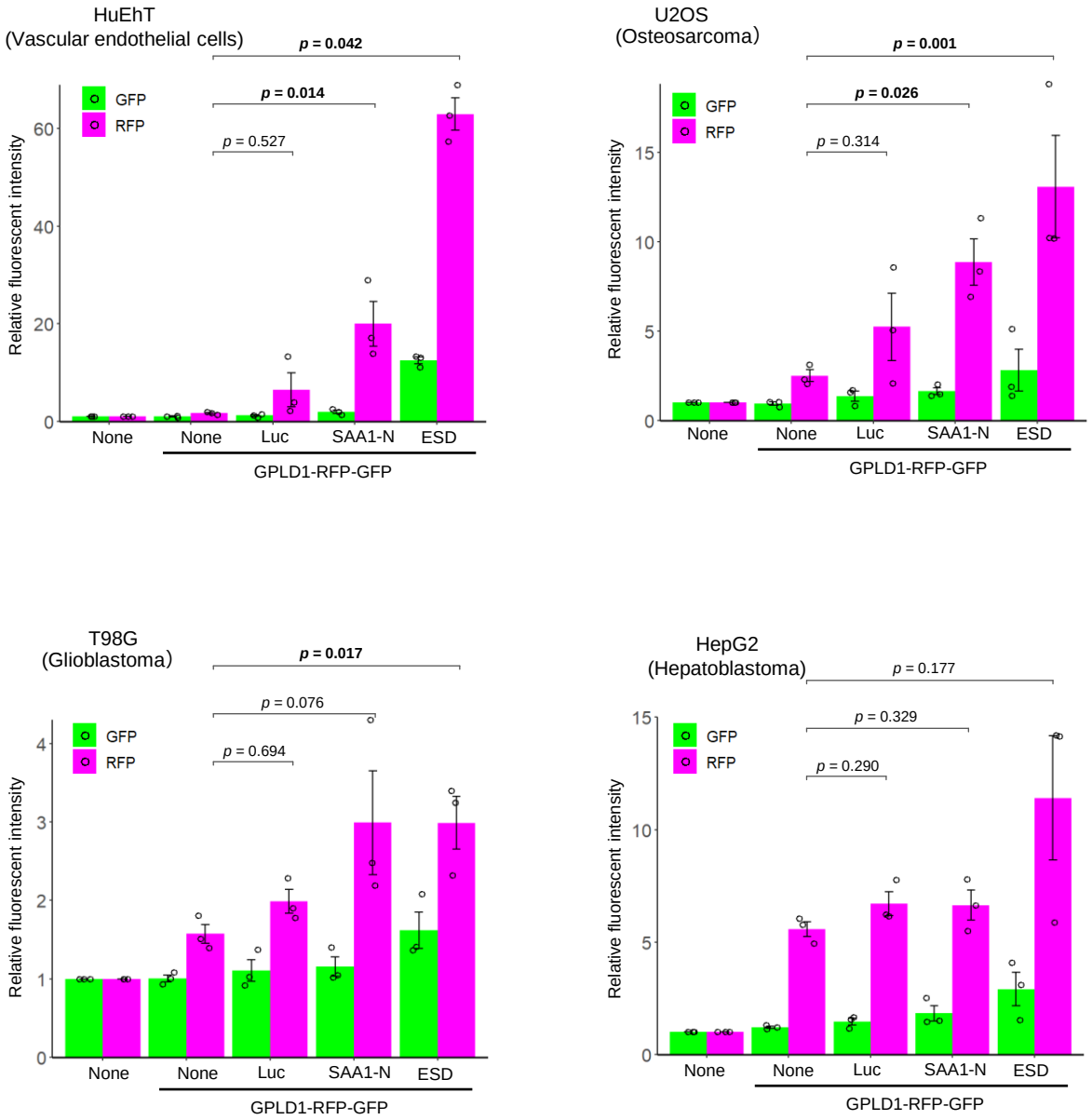

Figure S5. GPLD1-substrate complex is internalized in various cell lines

HuEhT, U2OS, T98G, and HepG2 were treated with medium containing GPLD1-RFP-GFP as described in Figs. 1B and 3A and analyzed by flow cytometry. The bar graph shows relative fluorescence intensities per cell normalized to untreated controls (n = 3). Data are presented as mean ± SEM. Exact p-values are also shown above the bars.

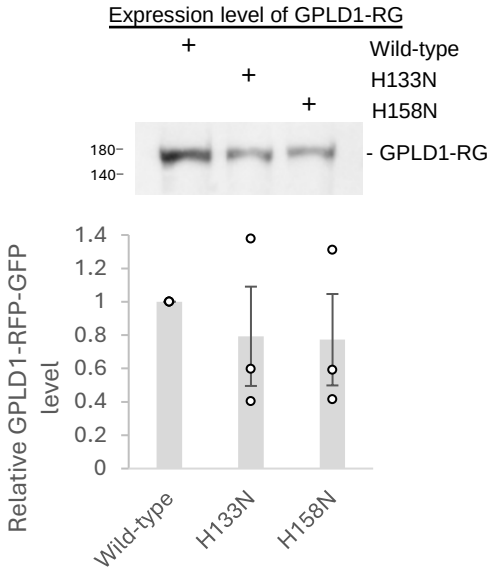

Figure S6. Expression level of GPLD1-RFP-GFP wild-type, H133N, and H158N

HEK293 cells stably expressing the indicated GPLD1-RG (wild-type, H133N, or H158N) were cultured for 4 days in serum-free Advanced DMEM/F12 medium supplemented with doxycycline. The conditioned media were analyzed by immunoblotting using an anti-GFP antibody. The observation that the GPLD1 catalytic mutants were secreted at levels comparable to the wild type suggests that their folding within the endoplasmic reticulum (ER) was not impaired. The relative band intensity is the -fold change of each sample's intensity, normalized to the intensity of wild-type, which was set to 1.0 (n = 3). Data are presented as mean ± SEM. Exact p-values are also shown above the bars.